Applications of Electrogenerated Chemiluminescence in Analytical Chemistry

Neso Sojic, Stéphane Arbault, Laurent Bouffier and Alexander Kuhn

Abstract The great success of electrogenerated chemiluminescence (ECL) in analytical chemistry can be measured by the widespread use of the technology in different fields, ranging from basic research to commercial clinical and biological applications. Indeed, this remarkable readout method offers intrinsic advantages by comparison with other transduction methods: high sensitivity, extremely wide dynamic range, and insensitivity to matrix effects. In addition, its versatility allows exploiting various types of biomolecular interactions and therefore to detect specifically targeted analytes of biological interest such as proteins, nucleic acids, and enzymatic substrates. Numerous assay formats, biosensors, or analytical strategies with new ECL labels or with label-free approaches have been proposed by using nanostructured materials: carbon nanotubes, metal or doped nanoparticles, graphene, carbon dots, quantum dots, or ultrathin films. The development of analytical ECL has also been fueled by discovering novel luminophores and efficient co-reactants and also by deciphering the complexity of the ECL mechanisms at the minute scale. The combination of ECL with microfluidics, paper-based materials, bipolar electrochemistry, and portable miniaturized devices has led to various intriguing and promising analytical applications.

1 Introduction

Electrogenerated chemiluminescence, also referred to as electrochemiluminescence (ECL), belongs to the family of luminescence phenomena in which the transition of an excited state of a luminophore (an atom or a molecule) to a state of lower energy is accompanied by the emission of photon [1, 2]. Such light-emitting events are classified according to the nature of the process providing the energy to reach the excited state. For example, in photoluminescence (i.e., fluorescence or phosphorescence),

N. Sojic (✉) · S. Arbault · L. Bouffier · A. Kuhn
Institut des Sciences Moléculaires, CNRS UMR 5255, University of Bordeaux, Bordeaux INP ENSCBP, Pessac, France
e-mail: Neso.Sojic@enscbp.fr

F. Miomandre and P. Audebert (eds.), *Luminescence in Electrochemistry*,
DOI 10.1007/978-3-319-49137-0_8

photoexcitation occurs by the absorption of photons by the luminophore. In chemiluminescence, the energy source is provided by the homogeneous chemical reactions between at least two reactive species. ECL is a specific case where these reactive intermediates are produced electrochemically at the electrode surface. Then, they undergo a chemical step characterized by a highly exergonic electron-transfer reaction generating the excited state of the luminophore. Light emission occurs during the relaxation to the ground state. So ECL is initiated by an electrochemical step, continues with a homogeneous chemical reaction, and ends with a photochemical step. It differs from electroluminescence which is the radiative recombination of electrons and holes in a material, usually a semiconductor. In addition, ECL can be considered as the competition between a light-emitting and a non-radiative transition in the Marcus inverted region [3]. Indeed, the energetic electron-transfer reaction occurring during the second step can actually favor excited-state formation over the ground-state formation. Therefore, ECL evidences the existence of an inverted Marcus region for electron-transfer reactions.

Since ECL combines electrochemical addressing and orthogonal optical detection modalities, it has attracted large interest in different fields such as photochemistry, electrochemistry, and analytical chemistry [4–9]. Due to its interdisciplinary nature and also to its remarkable characteristics, ECL has shown great achievements in fundamental research but also for practical applications, mainly in the diagnostic market with immunoassays [10–13]. For analytical applications, the information is contained in the light signal, and its intensity is directly proportional to the concentration of a limiting reactant involved in the ECL process. For example, the luminophore could be used as a label in a biorecognition chain, such as in immunoassays. Modern detectors can easily measure light intensity at very low levels which allows the development of ultrasensitive analytical methods based on ECL technology.

Compared with other sensing methods used in bioassays, ECL obviously does neither need any radio-isotope tracer nor optical excitation (photoluminescence-based methods), which avoids background from scattered light or sample auto-fluorescence. It just requires a photodetector and a potentiostat, which is a fairly light instrumentation favorable for its integration with fluidic approaches within high-throughput systems. From an analytical point of view, it offers many intrinsic advantages. First, extremely low detection limits can be reached for biomolecules (picomoles), in particular since ruthenium-based labels can be regenerated in situ at the electrode surface. As a result, many photons are produced per measurement cycle, which greatly enhances the sensitivity of the ECL technique. The most extensively investigated ECL luminophore is tris(2,2′-bipyridyl) ruthenium(II), $Ru(bpy)_3^{2+}$, which can be considered as an ECL standard. Second, if the luminophore is used as a label in the presence of an excess of co-reactant [14], an extremely wide dynamic range greater than six orders of magnitude may be achieved [15]. Third, since ECL is initiated by the application of a suitable potential at an electrode surface, it allows the time, the duration (application of the potential), and position (localized near the electrode surface) of the light-emitting reactions to be precisely controlled, which can improve the

signal-to-noise ratio. In addition, the control of the luminescence process in space enables multiplexed analyses using electrode arrays and imaging techniques. Fourth, ECL-active labels such as $Ru(bpy)_3^{2+}$ derivatives can be easily conjugated to biomolecules (e.g., proteins, peptides, and oligonucleotides) by coupling their amino reactive groups to the bipyridine—N-hydroxysuccinimide (NHS) ligands of the label. Fifth, ECL allows the simultaneous measurement of two experimental parameters versus potential (i.e., light intensity and Faradaic current), and thus a great selectivity and control over the light-emitting reactions. Combining both parameters yields also important insights in the ECL mechanisms. Sixth, it provides a fast time response, typically a few seconds. Finally, the reagents are very stable, and the reactive intermediates are electrogenerated in situ.

2 Principles of ECL

As already mentioned, ECL is the light emitted from an electronically excited state which is produced by energetic electron-transfer reactions. The earliest ECL reactions occurred by the annihilation reaction between species electrogenerated by pulsing the electrode potential [16–18]. However, they were limited to aprotic solvents. After the initial reports with aromatic hydrocarbons, the study of the remarkable electrochemical and ECL properties of the water-soluble $Ru(bpy)_3^{2+}$ luminophore was reported by Bard et al., and it represented a major breakthrough in the field [19, 20]. The reasonable stability of the oxidized form, $Ru(bpy)_3^{3+}$, in water paved the way to the discovery of ECL in aqueous phase. In the early 1980s, ECL was generated in aqueous solutions containing both $Ru(bpy)_3^{2+}$ and a co-reactant such as oxalate by applying a single anodic potential [21]. It opened a new area for ECL. Indeed, the large majority of ECL bioanalytical applications are based on a mechanism involving the reaction of a sacrificial co-reactant species with the luminophore. After a first report on chemiluminescence emission obtained by mixing $Ru(bpy)_3^{3+}$ and tri-*n*-propylamine (TPrA) [22], Leland and Powell described the use of TPrA as a very efficient co-reactant that generates strong ECL signals in aqueous solutions [23]. In the early 1990s, ECL bioassays were reported that led to the development of commercial ECL systems for immunoassays [10, 11, 24]. Considering all these developments, ECL mechanisms can be separated into two dominant pathways: the annihilation pathway and the co-reactant pathway.

2.1 Annihilation Pathway

In the annihilation pathway, an oxidized and a reduced species are electrochemically produced at the electrode surface by applying alternating pulsed potentials. Then, these two species react together according to an annihilation reaction to

generate the electronically excited state of the luminophore. It relaxes to the ground state and emits a photon. Depending on the available enthalpy of the annihilation reaction and of the energy levels of the luminophore, the possible mechanism for the ECL annihilation pathway can be presented as follows:

$$A - e^- \rightarrow A^{\cdot +} \quad \text{(oxidation at the electrode)} \tag{1}$$

$$A + e^- \rightarrow A^{\cdot -} \quad \text{(reduction at the electrode)} \tag{2}$$

$$A^{\cdot +} + A^{\cdot -} \rightarrow (2 - \alpha)A + \alpha {}^1A^* \quad \text{(formation of the singlet excited state)} \tag{3}$$

or

$$A^{\cdot +} + A^{\cdot -} \rightarrow (2 - \beta)A + \beta {}^3A^* \quad \text{(formation of the triplet excited state)} \tag{4}$$

$${}^3A^* + {}^3A^* \rightarrow (2 - \gamma)A + \gamma {}^1A^* \quad \text{(triplet-triplet reaction)} \tag{5}$$

$${}^1A^* \rightarrow A + h\nu \quad \text{(ECL emission)} \tag{6}$$

If the homogeneous electron-transfer reaction between the electrogenerated species is exergonic enough, the annihilation process leads directly to the emitting singlet excited state of the luminophore (Eqs. 1–3). In this case, the system has sufficient available energy and the emitted ECL follows the singlet route, also called "S-route." But, if the enthalpy of the annihilation reaction is insufficient to populate directly the singlet state, the system may follow the "T-route" where the triplet state is first produced (Eq. 4). For such an "energy deficient system," triplet–triplet annihilation may eventually yield the singlet emitting state in a second step (Eq. 5). Both routes have been extensively studied with various systems [25, 26].

2.2 *Co-reactant Pathways ("Reductive–Oxidative," "Oxidative–Reductive")*

An alternative mode of ECL generation with more complex mechanistic pathways is based on the use of sacrificial co-reactants (e.g., oxalate, TPrA, peroxydisulfate, benzoyl peroxide (BPO),…). A co-reactant can be defined as a chemical species that, upon electrochemical oxidation or reduction, produces very reactive intermediates capable to react with the oxidized or reduced luminophore to generate the desired excited state. The corresponding mechanisms are often referred to as "oxidative–reductive" ECL and "reductive–oxidative" ECL, respectively [4]. The method is very simple, because it requires just the application of a single potential step. An example of an "oxidative–reductive" co-reactant is the oxalate ion that was

the first ECL co-reactant discovered in water [21]. The luminophore $Ru(bpy)_3^{2+}$ and the co-reactant $C_2O_4^{2-}$ are both oxidized at the electrode surface. Then, upon bond cleavage, $C_2O_4^{\cdot -}$ forms a strong reducing species ($CO_2^{\cdot -}$) that reduces $Ru(bpy)_3^{3+}$ and generates $Ru(bpy)_3^{2+*}$, which emits light. Thus, ECL mechanism of oxalate is often referred to as an "oxidative–reductive" route because the sequences of the electron-transfer reactions are as follows: (1) The electrochemical oxidation at the electrode surface and (2) the reduction of the oxidized luminophore by the radical. Another example of an "oxidative–reductive" system is the model $Ru(bpy)_3^{2+}$/TrPA system which is considered as a standard in ECL. ECL mechanism of $Ru(bpy)_3^{2+}$ with amine-based co-reactants [14, 27] depends on a great variety of parameters: nature of the co-reactant, electrode material, solvent, pH, presence of surfactant in the solution, respective concentrations of the co-reactant and of the ruthenium complex, and hydrophobicity of the electrode surface. For example, at high concentrations of $Ru(bpy)_3^{2+}$ (> 0.1 mM), the "catalytic route" (also called "EC" route) is the dominant process for ECL [28–30]. Along this path, the catalytic oxidation of TPrA occurs by a reaction with electrogenerated $Ru(bpy)_3^{3+}$. In the commercialized bead-based immunoassays, the luminophore is used as a label and is immobilized on the bead surface. In this case, ECL follows the "revisited" route where only TPrA is oxidized at the electrode surface [31]. The resulting radicals, $TPrA^{\cdot +}$ and $TPrA^{\cdot}$, diffuse to react with the luminophore [32], as detailed in the Sect. 4 and also in the Chapter "Theoretical Insights in ECL" by Amatore et al. Most of the co-reactant ECL reports are based on the "oxidative–reductive" scheme because it operates efficiently in water. Indeed, it just requires imposing a simple anodic potential and also oxygen evolution is very slow in aqueous solutions. Therefore, it does not interfere significantly with the ECL generation.

For the "reductive–oxidative" route, the situation is completely different in aqueous solutions because very cathodic potentials are required. Thus, hydrogen evolution dominates and the electrogenerated species decompose too rapidly to obtain a stable ECL process. However, in pure organic solvents or mixed acetonitrile/water solutions, strong ECL intensity may be generated by using peroxydisulfate or BPO as co-reactants. First, the co-reactant is reduced simultaneously with the luminophore at the surface of the electrode. After dissociation, the peroxydisulfate or BPO co-reactants produce strong oxidants $SO_4^{\cdot}$ or $Ph\text{-}CO_2^{\cdot}$, respectively, which oxidize the reduced luminophore to generate the excited state. Finally, radiative de-excitation generates the ECL emission.

To select efficient co-reactants giving strong ECL intensity, a number of criteria should be fulfilled: solubility, low oxidation or reduction potentials, stability, toxicity, kinetics, quenching effects, low ECL background, adequate redox potentials, and sufficient lifetimes of the radicals.

3 Analytical Strategies

As stated in the previous section, ECL is intrinsically based on a sequential combination of electron transfers, chemical steps, and light emission. Three key elements can be potentially tuned in order to achieve ECL: the nature of the luminescent moiety, the interface where the electron-transfer steps take place, and the chemical mechanism allowing the formation of the excited state. This section will focus on the main analytical possibilities that were historically reported to design ECL-sensing strategies.

3.1 Co-reactant ECL (Co-reactant is the Analyte)

ECL could be promoted according to either annihilation or co-reactant pathways. By employing the same luminophore, various co-reactants can be used in order to generate ECL following reductive–oxidative or oxidative–reductive mechanisms. The amount of light generated at the electrode–solution interface directly depends on the concentration of the dye [33] but also of the co-reactant [23]. Therefore, any ECL-active co-reactant can be potentially detected and quantified as its concentrations will directly influence ECL intensity.

For example, the determination of oxalate in aqueous solutions was reported as early as in 1983 with an ECL intensity varying linearly over a concentration range between 1 and 100 μM [34]. Such concentration values are compatible with the level typically found in normal human blood or urine samples. In a more recent study, the quantification of oxalate was directly performed from urine and plasma samples by combining reversed-phase ion pair HPLC with an ECL readout [35]. The detection limit was found to be below 1 μM corresponding to an injection of only 25 pmol. The calibration curve for oxalate was linear throughout the entire clinical range, and the concentration values were compared with a conventional enzymatic method with a discrepancy lower than 1%.

Peroxydisulfate concentration was also measured accurately when used as a co-reactant for $Ru(bpz)_3^{2+}$ cathodic ECL (with bpz = 2,2′-bipyrazine). The method is highly specific with an impressive linear range over six orders of magnitude of concentration between 1 nM and 1 mM when a rotating disk is used as the working electrode [36]. Pyruvate was equally determined in a comparable manner with $Ru(bpy)_3^{2+}$ anodic ECL in the presence of cerium nitrate, increasing the diversity of possible ECL analytes [37]. The limit of detection (LOD) was found to be about 0.3 μM (equivalent to 27 ppb), and the interference of various chemicals such as EDTA and citrate was eliminated because of their presence in potential samples from fermentation media.

Tertiary and secondary amines can be quantified without chemical modification or derivatization by taking advantage of ECL reaction, typically with $Ru(bpy)_3^{2+}$

used as an effective luminophore. However, many tertiary amine compounds are capable to produce intense ECL, whereas others do not generate significant light emission. In that context, a remarkable structure/activity relationship study was published a decade ago by Knight and Greenway [38]. The key chemical features have now been clearly identified in order to rationalize the corresponding ECL proficiency. First, the presence of a hydrogen atom on the carbon in position α is essential for the radical formation regardless the mechanistic pathway. Electron-withdrawing groups such as carbonyl, hydroxyl, or halogen located on the amine will destabilize the radical intermediate and therefore drop down ECL emission. The presence of electron-donating substituents will contrarily favor the radical stabilization and increase the resulting ECL activity. This is in fact a very classic reactivity trend based on the stabilization of the radical intermediates which hinders subsequent reactivity and thus reduces ECL accordingly.

Relevant examples illustrating this structure/activity relationship could be briefly mentioned. A direct comparison of the ECL emission recorded with mono-, di-, and tri-propylamine reveals a marked increase from 4 to 48 and 660, respectively (given in arbitrary units) [39]. This implies that changing from a tertiary to a primary amine could potentially lower ECL by a factor up to 165. Also, the following trend Phenyl > Hydroxy > Chloro in the ethylamine series is well explained by the electron-withdrawing ability. Indeed, phenylethylamine is almost four times more efficient than chloroethylamine which directly correlates with the Hammett substituent constant [40]. Another more quantitative method to predict ECL efficiency of various alkylamines was also previously reported based on the redox potential value of the reducing intermediate involved in the charge-transfer steps leading to the excited state [22]. The reader should be aware that the comparison between co-reactant and the prediction of relative ECL intensity based on the corresponding molecular structure should be made with caution. Indeed, several effects that may be antagonist may influence the ECL strength like the respective oxidizing/reducing power of the reactive intermediates as well as their relative stability. This is why a comparison between structurally related molecules seems only reasonable especially with complicated co-reactants exhibiting several functional groups. For example, the superior ECL capability of 2-(dibutylamino)ethanol compared to TPrA was nicely reported by Liu et al. [27], and the enhancement is due to the promotion of amine oxidation thanks to the presence of the hydroxyethyl group.

The most common anesthetic drugs exhibit a chemical structure combining a tertiary amine and an aromatic moiety connected together either by an amide or an ester bonding (Fig. 1). Thus, the presence of the amine moiety makes them suitable for ECL determination. The ECL activity directly matches the chemical structure of the anesthetics. Indeed, bupivacaine (also known under the brand name Marcaine) exhibits the higher ECL intensity (100% a.u.) thanks to its long alkyl groups, whereas the signal recorded for lidocaine and tetracaine, in the same conditions, steadily decreases to 63 and 16% because of the shorter ethyl and methyl groups, respectively [38].

It is also noteworthy that many NADH-dependent enzymatic processes have been measured by ECL because the NADH coenzyme contains an amine group

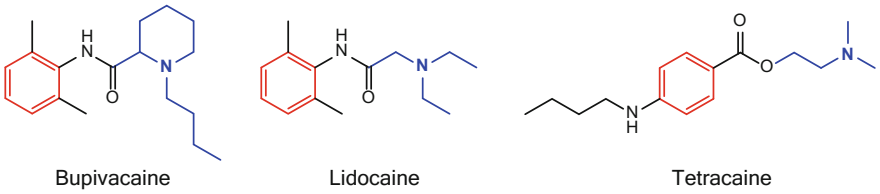

Fig. 1 Chemical structures of local anesthetics with the aromatic ring drawn in *red* and the tertiary amine in *blue* [38]

which can act as a co-reactant for $Ru(bpy)_3^{2+}$ ECL, whereas NAD^+ does not behave as a co-reactant [41]. Such strategies will be detailed below in Sect. 4.

3.2 *Luminophore ECL (ECL Labels)*

It was already mentioned that the ECL intensity depends on the concentrations of both emitter and co-reactant. However, almost all practical applications in biomedical diagnostics are performed under experimental conditions where the ECL intensity is directly proportional to the luminophore amount. Also, the only ECL dye used in commercial assays is the $Ru(bpy)_3^{2+}$ complex which exhibits a strong ECL efficiency. It is readily available and can be further chemically functionalized. In the latter cases, $Ru(bpy)_3^{2+}$ is covalently attached to one of the biochemical species involved in the recognition process which is the so-called ECL labeling strategy. Then, the ECL is promoted in the presence of a large excess of co-reactant (generally TPrA) in order to be only sensitive to the dye content either in solution or surface-immobilized structures. In this strategy, the emitter is chemically bound to the analyte which allows a proper quantification. ECL is a very useful toolbox for molecular diagnostics which necessitates low-concentration detection of various bioanalytes and markers, especially when diseases are at an early stage of development. Many different biomolecules need to be detected including DNA, RNA, peptides, proteins, or specific antibodies. Therefore, the two most classic chemical labeling processes include the presence of an activated ester such as NHS linked to the ruthenium complex or a phosphoramidite conjugate (Fig. 2). The former reacts with primary amines to form an amide bond, which is useful in the case of biomolecules containing amino acids, whereas the latter allows incorporating the label into oligonucleotides.

The detection of DNA with ECL labels as well as the development of immunoassays has been established in practical clinical diagnostic more than 25 years ago [11]. In fact, the use of ECL labeling based on ester bond formation through NHS activation was first reported in DNA assays back in 1991 [42]. This opened the door to numerous applications for the rapid detection of polymerase chain reaction–amplified products from specific genes or viruses. More recently,

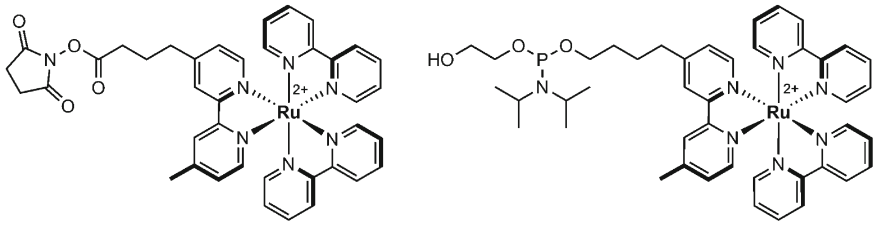

Fig. 2 Chemical structures of $Ru(bpy)_3^{2+}$ luminophore conjugated with an activated ester (*left*) or a phosphoramidite (*right*) for ECL labeling of various biomolecules [7]

ECL labeling was also used to evaluate the surface coverage of biosensors, especially for immobilized DNA and protein [43]. The strategy adopted in some recent contributions in the field of DNA biosensors combines ECL labeling and detection with supramolecular assembly such as hairpin [44] or aptamer folding [45] for the selective detection of small molecular targets.

The transduction of antigen/antibody recognition is by far the largest application of ECL. This strategy used generally the classic $Ru(bpy)_3^{2+}$/TPrA system where the dye is used as a label to report the immune affinity. This was applied to a wide variety of assays which relate the emitting label to analyte concentration such as β-amyloid peptide, insulin, interleukins, or various cancer antigen markers. This field was reviewed in detail by several authoritative reviews from Richter [7], Miao [4], and Liu et al. [9] and will be discussed in Sect. 4.

3.3 NP-Based ECL

The promotion of ECL at the surface of nanoparticles is an emerging and very promising field. The general idea is to position semi-conducting particles at the electrode surface to allow the injection of excitons either in the valence band or conduction band of the quantum dots (QDs). Several mechanistic pathways can be followed by using appropriate co-reactants in order to generate either anodic or cathodic ECL (Fig. 3). This area of ECL has been extensively reviewed recently by the group of Wu et al. [46] and Zhao et al. [47]. Therefore, in this subsection, the attention will be solely focused on the historical publications.

The very first contribution was introduced by Bard with silicon nanocrystals with a size ranging between 2 and 4 nm in diameter [48]. Indeed, the electrochemical gap between the onset of electron and hole injection expands with decreasing particle size. The ECL spectra recorded in solution feature a significant redshift compared to photoluminescence (PL) with a maximum centered at 640 nm against 420 nm, respectively. This first seminal work was followed by a series of contributions exemplifying the versatility with plenty of different QDs such as 3 nm in diameter CdSe prepared from Cd-acetate and Se powder [49]. The same typical

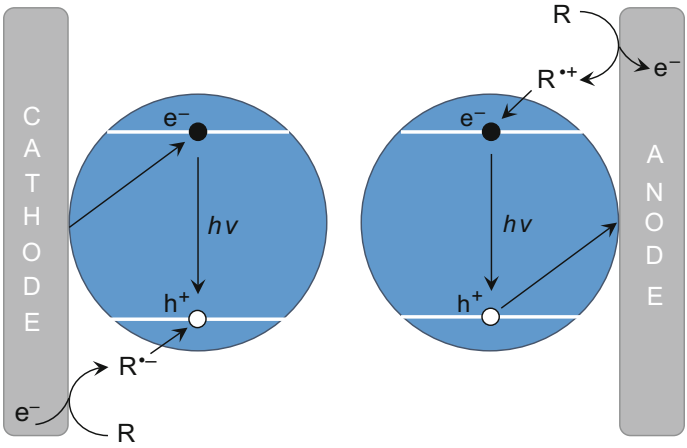

Fig. 3 Scheme of ECL promotion with QDs. The excitons (*holes and electrons*) are injected by electrode and co-reactant following the cathodic or anodic pathways [46]. Reprinted with permission from Ref. [46]. Copyright 2014 American Chemical Society

redshift of ~200 nm with respect to PL spectrum was assigned to the implication of surface states in the emission process. CdSe was also used later as an ECL-active nanocrystal film employed for sensing applications in aqueous solution. This was illustrated for the detection of H_2O_2 co-reactant with a typical LOD of 10^{-7} M [50]. ZnSe [51], CdTe [52] or CdS [53] have also been reported. These QDs are either used alone or in combination with other classes of materials in order to prepare composites with tunable properties or enhanced surface area (see next section). QDs have then been used to prepare modified electrodes and tested as ECL biosensors for low-density lipoprotein (LDL). The LDL concentration was measured through the decrease in ECL signal resulting from the binding to a specific receptor with an outstanding 6 ng L^{-1} LOD [53]. Another analytical strategy involving ECL energy transfer to analytes was also demonstrated [54]. In the latter case, the energy transfer takes place from the excited CdTe QDs to quencher catechols such as dopamine or adrenalin as model analytes with a linear response of 4 orders of magnitude from μM to nM range, typically.

Apart from these transition metal-based QDs, carbon-based semiconducting systems have also been described. ECL spectra of carbon nanocrystals released from graphite were measured with a maximum wavelength of both anodic and cathodic processes centered at 535 nm [55]. Most of the time, expensive techniques such as laser ablation or proton beam irradiation are employed, as well as harsh chemical degradation approaches from various carbon sources. However, it is noteworthy that a facile microwave-assisted pyrolysis synthesis of fluorescent and ECL-active carbon nanoparticles has been performed in a matter of minutes [56]. The size is adjusted by the synthesis duration and reasonable monodispersity was achieved with particles exhibiting between 2 and 4 nm in diameter. Two-color

graphene QDs with a greenish-yellow luminescence were reported for the very first time recently [57]. The ECL mechanistic pathway was studied together with an application to Cd^{2+} sensing based on ECL quenching by cysteine as masking agent.

Noble metal clusters constituted by a few atoms have also been recently investigated by Hesari et al. [58]. Such ultrasmall chemical entities exhibit properties that are close to a single molecule behavior. Several clusters such as Au_8, Au_{25}, and Au_{38} have been discussed in the literature. In particular, the ECL emission is remarkable in the near-infrared region with a fundamental mechanistic study which is now well-established [59]. It is also noticeable that, for the Au_{38}/TPrA system, the ECL yield is 3.5 times higher than the reference $Ru(bpy)_3^{2+}$/TPrA one [60]. The cathodic ECL of Au_{25} nanoclusters with $K_2S_2O_8$ as co-reactant deposited on an ITO electrode was used for the detection of dopamine, and this contribution opened the door to new promising material platforms for ECL biosensors [61]. Finally, the photophysical properties of silver nanoclusters consisting of only a few metal atoms were also reported. They exhibit both tunable photo- and electro-chemiluminescence such as solvatochromism because of a dramatic sensitivity to the local chemical environment [62].

3.4 Nanomaterials ECL

The development of efficient and sensitive ECL platforms for chemical or biochemical sensing became regularly more sophisticated thanks to the design of complex modified surfaces and architectures [63]. This area is currently rapidly expanding as it combines and takes benefit of surface-immobilized structures based on nanoparticles, nanotubes, and polymer or metal complexes thin films.

The initial works were simply done by immobilizing $Ru(bpy)_3^{2+}$ alone [64] or inside Nafion on an electrode surface for the preparation of a regenerable ECL-active layer [40, 65]. Later, the combination of Nafion-doped sols was found to show even better properties. The amount of cationic luminophore exchanged into these films strongly depends on the proportion of each chemical ingredient in the mixture. The ECL response was studied with TPrA or sodium oxalate as co-reactant, and greater ECL emission was recorded in the composite Nafion/silica films when compared to Nafion only [66]. Such a strategy was generalized from SiO_2 to TiO_2 sol/gel with enhanced ECL capability [67]. The optimal composition ratio for ECL was found to be 50% Nafion content and the corresponding modified electrode was studied for co-reactant titration with typically μM (oxalate) and sub-μM LOD (TPrA). The ECL sensor was also combined with HPLC for the determination of erythromycin in human urine samples. Direct incorporation of $Ru(bpy)_3^{2+}$ dye inside SiO_2 NPs casted onto electrode surfaces provides a new generation of multilayer ECL-active films [68]. The corresponding films showed improved linearity of the signal as a function of the analyte concentration and enhanced stability due to the multilayer architecture and high-active surface area.

This sensor was then further optimized to achieve up to 3 nM LOD for TPrA which is 3 orders of magnitude lower than the benchmark Nafion-based ECL sensor with long-term stability [69].

QDs have been extensively developed in combination with several forms of nanomaterials in order to obtain synergetic effects. For example, a novel strategy was developed by combining CdSe nanocrystals, carbon nanotubes, and chitosan biopolymer [70]. A label-free ECL sensor for the detection of human immunoglobine antibody (IgG) was built up. All these ingredients put together allow biocompatibility and more importantly a large surface area generating a 20-fold higher ECL intensity for enhanced sensitivity. The interaction between surface plasmons of Au metal nanoparticles and ECL-active semiconducting particles such as CdS QDs was also evidenced. This was illustrated with CdS thin films for the ultrasensitive detection of thrombin aptamer [71]. The multifunctional system showed up to a 5-fold ECL signal increase when compared to that without the incorporation of Au NPs with an outstanding linearity range from 0.1 to 100 fM. The amplification of ECL based on a QDs platform for the sensing of antioxidants was achieved with graphene oxide [72]. In fact, the latter facilitated the promotion of excitons inside CdTe QDs and triggered the generation of reactive oxygen species, thus leading to a large ECL enhancement. Glutathione peptide was selectively detected at μM concentration, even in the presence of thiol-containing competitors such as cysteine. Another system constituted by a polymer-protected graphene with Au and CdSe nanoparticles composite was successfully combined for the detection of IgG [73]. The advantage of plasmonic particles with an improved surface area offered an impressive linearity response over 6 orders of magnitude with a LOD of 5 pg L^{-1} for ultrasensitive protein detection. The same trend was equally observed with functionalized graphene and gold nanorods multilabeled with an enzyme such as glucose oxidase (GOx) and secondary antibody [74]. Luminol was used as an ECL-active luminophore, and the whole system was applied to the detection of prostate specific antigen (PSA) protein, a biomarker of prostate cancer. The multifunctional platform works through a cascade of amplifications of luminol ECL in the presence of glucose and oxygen and pg mL^{-1} of PSA is detectable in such conditions.

To summarize, the design of surface-modified electrodes combining intimately nanomaterials and plasmonic effects [75–77] is very promising for point-of-care diagnostics, especially in the context of clinical screening of trace biomarkers.

3.5 Bipolar ECL Detection

Bipolar electrochemistry (BPE) has attracted in the last few years an exponentially increasing interest in the scientific community due to some unique features, which can also be of primary importance in the context of ECL. The concept is less well known than classic electrochemistry where a conventional three-electrode setup, composed of a working, counter, and reference electrodes, is used [1]. In such a

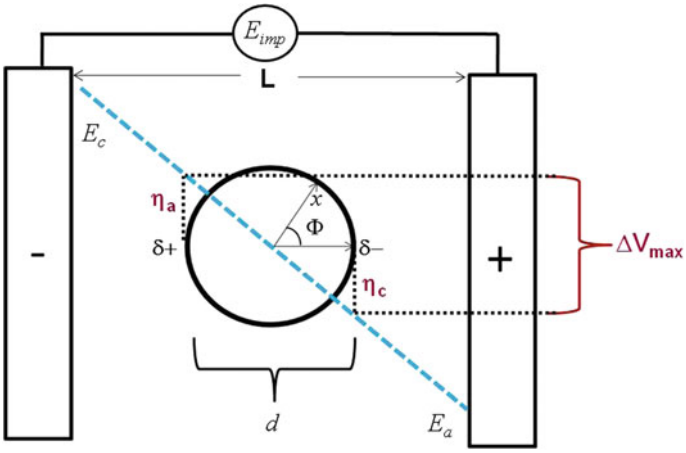

Fig. 4 Polarization of a conducting object. Scheme illustrating the 2D projection of the polarization of a spherical conducting object located between two feeder electrodes in a solution

normal electrochemical setup, the electrode of interest is the working electrode, where, depending on its polarization with respect to the solution, either an oxidation or a reduction reaction occurs. For BPE, things are slightly different, because both oxidation and reduction reactions occur simultaneously on the same electrode, which is not physically connected to a power supply through an electric contact.

A straightforward way to generate a bipolar electrode is to place a (semi)conducting object in a solution in which an electric potential gradient exists, generated by two feeder electrodes which are not in physical contact with the immersed object. As the conducting object is by definition equipotential, it will experience an inhomogeneous potential difference with respect to the solution. This will automatically lead to a situation where some parts of the object are more likely to undergo an oxidation reaction, whereas other sections will become preferential sites for a reduction reaction (Fig. 4).

As a consequence of the presence of this electric field, individual anodic and cathodic polarisation potentials η_a and η_c will be established at every point of the object. Depending on the localisation x on the surface of the object, these potentials vary and can be calculated as:

$$\eta_x = \mathrm{E}\frac{d}{2}\cos\Phi \tag{7}$$

for a spherical object, with d being the object diameter and $\mathrm{E} = E_{imp}/L$ the electric field. As shown in Fig. 4, the maximum polarization potential difference occurs between the extremities of the object, and its value, $\eta_a - \eta_c = \Delta V_{max}$, can be calculated as:

$$\Delta V_{\max} = \text{E}d \tag{8}$$

This value directly induces the reactivity at the extremities of the polarized interface which can be used for many different applications [78, 79], and among others also to generate ECL. In terms of application of this concept to the detection of analytes, three main routes can be followed:

- either the analyte is simultaneously also a co-reactant of the ECL reaction (direct bipolar ECL reporting via oxidation of the analyte)
- or the analyte is detected by a reduction reaction, which is coupled through the bipolar electrode to the oxidative ECL reaction (indirect bipolar ECL reporting)
- or the analyte is indirectly involved in the ECL process such as, for example, by quenching the excited state

Manz and co-workers explored for the first time the possibility to use BPE for triggering ECL by following the direct detection route [80]. In their experiments, a photodetector measured remotely the ECL emission generated at a bipolar electrode, and it was shown that the electrochemical activity is directly related to the ECL intensity (Fig. 5a, b). This fits perfectly the requirements for performing analytical BPE, since an electrochemical reaction occurring on the bipolar object is correlated with, and transduced into, an optical signal. The second indirect route has been mainly investigated by Crooks and co-workers during the last decade and

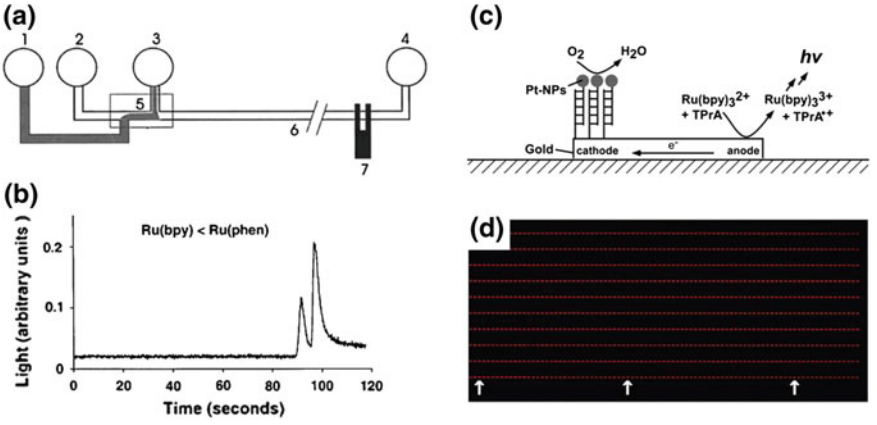

Fig. 5 Experimental illustration of the difference between direct and indirect bipolar ECL reportings. **a** Layout of a microfluidic device: *1* sample reservoir; *2* buffer reservoir; *3* sample waste; *4* buffer waste; *5* double-T injector; *6* separation channel; *7* bipolar detection electrode. **b** Electropherograms for $Ru(bpy)_3^{2+}$ and $Ru(phen)_3^{2+}$ separation with direct bipolar ECL detection [80]. **c** Scheme of indirect bipolar ECL reporting of DNA hybridization based on the coupling of the Pt-catalyzed reduction of oxygen on one side with the oxidation of the ECL ingredients on the other side of a bipolar electrode [81]. **d** A typical array of bipolar ECL electrodes with a density of 2000 recording elements per cm^2 [82]. Adapted with permission from Refs. [80–82]. Copyright 2009 American Chemical Society

established them as the leader of BPE-based sensing in general due to their pioneering work describing various bipolar configurations for such applications [78]. In the reported experiments, they used reduction reactions for the sensing event and oxidations as reporter reactions, many of them being based on ECL, simply because it offers an easy visual readout (see Fig. 5c, d). The seminal contributions of this group demonstrated that ECL generation at the vicinity of a bipolar electrode is a very simple and useful way to detect and quantify a spatially delocalized reaction, and therefore the concept has subsequently also been extensively exploited by many other groups in the last few years [83–94].

From a more theoretical point of view, some constraints are related to the use of the bipolar ECL approach. In order to observe ECL emission on a bipolar object, an adequate potential difference between the solution and its two poles has to be induced. Considering the classic $Ru(bpy)_3^{2+}$/TPrA system, its oxidation at the anodic side of the object requires at least a potential of E_{ox} = 1 V versus Ag/AgCl. On the other hand, a reduction reaction has to occur simultaneously at the cathodic pole with equal intensity. For the case of an aqueous system (pH 7.4), this will involve the reduction of protons, which takes place, for example, on carbon typically at E_{red} = −1.1 V versus Ag/AgCl. Therefore, ECL can only be generated if the polarization potential difference ΔV between both extremities of the bipolar electrode is at least equal to $|E_{red} - E_{ox}| = 2.1$ V. Taking into account Eq. 8 from above, this means that a minimum global electric field between the feeder electrodes of $E = 2.1\ V/d$ is needed to observe ECL emission on an object with a characteristic dimension d. For very small objects, this can be a drawback, because very high absolute voltages (of the order of kV or more) might be necessary to trigger the ECL reaction for a given experimental setup. On the other hand, one of the undeniable advantages is that ECL can be generated on an object without direct electrical connection, and thus it is also possible to address thousands or millions of objects simultaneously with just two feeder electrodes. These latter aspects open the door to some completely new applications of ECL [83, 90], like the emission of light from moving objects [95, 96], or the generation of light in the bulk of a solution (Fig. 6) [97, 98].

All these very appealing features allow envisioning the development of low-cost high-throughput screening methods based on various already well-established analytical concepts such as DNA (de)hybridization [94] or enzymatic reactions [87, 99] when combining them with a bipolar electrochemical setup.

4 Analytical Applications

The main applications of all the methodological and chemical systems described above are dedicated to bioanalyses. These applications can be divided into three main types and objectives: the immunoassays, DNA analyses, and more recent aptamers and DNAzymes detections. The immunoassays are the major ones, not

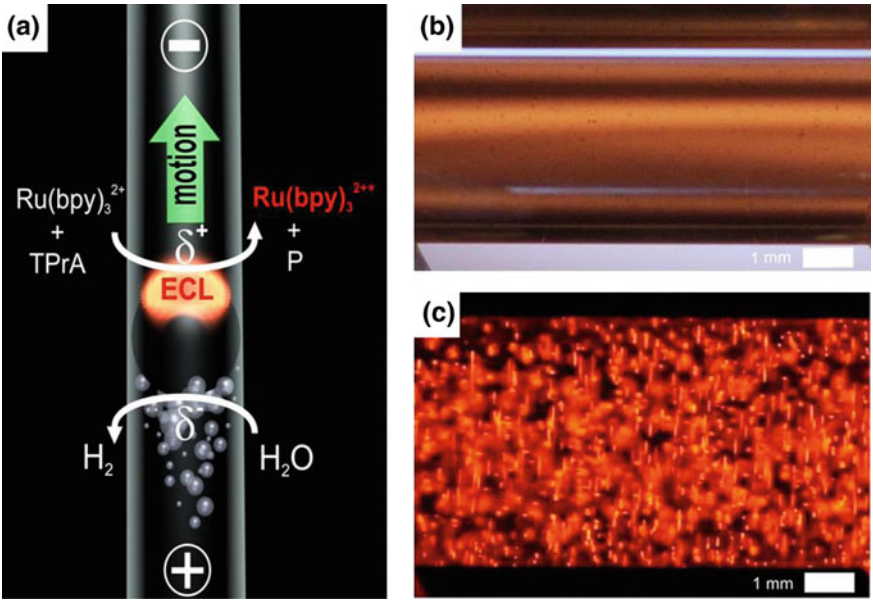

Fig. 6 **a** Scheme of a light-emitting bipolar electrochemical swimmer. Concomitant reduction of H_2O at the cathodic pole (*bottom of the bead*) and oxidation of ECL reagents at the anodic pole (*top of the bead*) induces simultaneous motion and light emission in a glass capillary [95]. **b** Bulk bipolar ECL emission from a suspension of carbon nanotubes (CNTs) in a capillary. Images of the suspension of CNTs **b** under *white light* without electric field and **c** in the *dark* of the bulk ECL emitted by the CNTs in the presence of electric field [97]. Reprinted with permission from Ref. [95]. Copyright 2012 Wiley. Reprinted with permission from Ref. [97]. Published by The Royal Society of Chemistry

only from the number of literature reports, but rather because of massive daily use for clinical diagnostics.

4.1 ECL Immunoassays

The pioneer works in ECL immunoassay (ECLIA) was done in particular by Bard and Whitesides [24], owing to a newly synthesized ruthenium chelate having a NHS residue. Thus, the availability of an efficient ruthenium label for bio-macromolecules (proteins, nucleic acids) has rendered possible the development of highly sensitive ECL bioassays [11, 42].

ECL immunosensing is mainly carried out in solid-phase heterogeneous formats, including direct, competitive, and sandwich immunoassay modes; the most common mode being the sandwich-type immunoassay [4, 13, 43]. In all types of heterogeneous immunoassay, the primary antibody (Ab1) is immobilized on the solid phase. In this case, the antibody must remain reactive after being adsorbed or

linked to a solid surface and must retain its structural integrity. Several approaches have been reported to immobilize this primary antibody: the covalent binding through glutaric dialdehyde [100], via L-cysteine [101, 102], via silanization [103] or 3,4,9,10-perylene-tetracarboxylic acid [104]. Besides, the sandwich-type ECLIA involves the conjugation of a secondary antibody (Ab2) labeled with the luminophore, typically a ruthenium complex.

Most of the commercial ECL-based systems for bioassay reported so far are based on the capture at the electrode surface of magnetic beads (a few microns in diameter), on which the immuno-complex formation occurs (Fig. 7). The major advantages of beads as a support are their greater surface area than the flat electrode surface, and the easy concentration of reacting beads by a magnet positioned below the electrode. In addition, it avoids the covalent immobilization of the biomolecules on the electrode surface which allows analyzing sequentially different samples with a high throughput. In the commercial Elecsys systems (Roche Diagnostics Inc.), conventional antigen–antibody reactions are achieved on the surface of streptavidin-coated paramagnetic microbeads owing to biotinylated antibodies. The ECL reaction then occurs on the bead surface between the TPrA co-reactant oxidized at the electrode, and the immobilized ruthenium label. More than 80

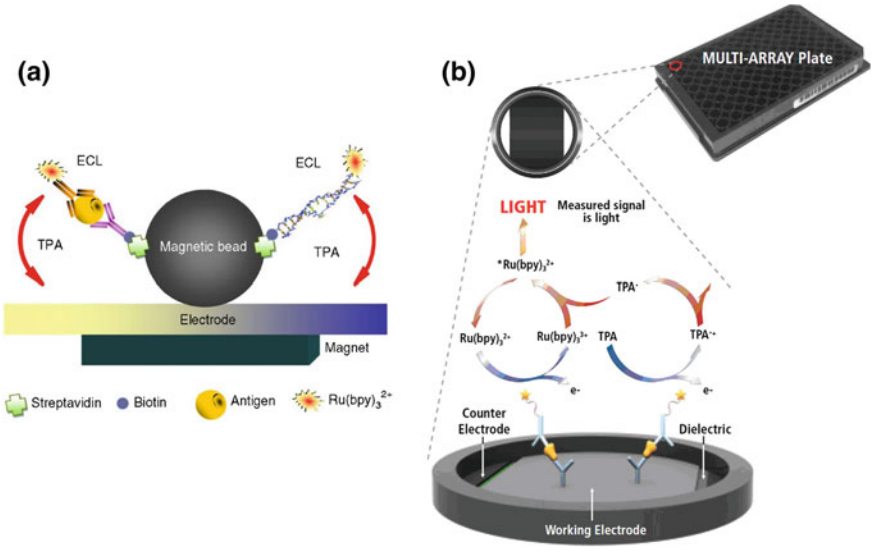

Fig. 7 Two major methodological approaches involved in commercial ECL bioassays. **a** Scheme of the sandwich immuno- and nucleic acid assays achieved on the surface of magnetic beads modified with either a target antibody or nucleic acid (streptavidin–biotin linkage) [12]. The secondary antibody or nucleic acid probes are labeled with $Ru(bpy)_3^{2+}$ moieties. ECL occurs owing to the immobilization of the microbead on the electrode surface under the effect of a magnet, and following addition of TPrA. **b** Scheme of the multiarray system integrated in a titer plate, based on sandwich immunoassays at the surface of a carbon electrode. Several sensors exist within each well allowing multi-ECLIA. Adapted from image by Meso Scale Diagnostics Inc.

bioassays are currently available with these systems, including cardiac markers, tumor markers, bone markers, infectious disease, thyroid function tests, anemia, and fertility tests (Roche Diagnostics Inc.). Recently, a new class of imaging-based ECL devices has been commercialized by Meso Scale Discovery Inc. (MSD). MSD systems are based on the immobilization of antibodies on electrodes and afford a multiarray technology. It uses the carbon-type electrode surface for bioaffinity binding assays, integrated into the bottom of 96-well microtiter plates, since the carbon surface has a 10-fold greater binding capacity than polystyrene. The binding reagent is immobilized on the carbon electrode plate surface, the ECL label (NHS-Ester tagged) is captured on the electrode via the binding complex, and finally the light is collected by a CCD camera. MSD ECLIA can be multiplexed by spotting up to 10 different antigens onto discrete areas of the carbon electrode within each well of the plate.

Understanding the excellent sensitivity of the ECL bead-based immunoassays is essential for further applications and it requires deciphering the ECL mechanisms of the model $Ru(bpy)_3^{2+}$/TPrA system. Different competitive mechanistic pathways have been proposed by Miao et al. [31]. They involve cascades of reactions of short-lived radicals with different redox potentials and reactivity at the minute scale [105] which is challenging to simulate accurately in solution phase (see Chapter "Theoretical Insights in ECL" for a detailed description). They can be classified into two main groups depending on how $Ru(bpy)_3^{2+}$ is oxidized. The first one requires the heterogeneous oxidation of $Ru(bpy)_3^{2+}$ at the electrode surface. However, these mechanistic routes cannot account for the ECL features reported at low oxidation potentials and also for the sensitivity of the bead-based assays [106–108]. Indeed, in this case, only the $Ru(bpy)_3^{2+}$ labels located on the bead within electron tunnelling distance from the electrode surface would be directly oxidized, meaning that an infinitesimal fraction of labels would contribute to the ECL signal following these paths. A second "revisited" route involving the mediated oxidation of $Ru(bpy)_3^{2+}$ by the cation radical ($TPrA^{\cdot+}$) has been proposed to explain how ruthenium centres located at micrometric distances from the electrode might generate ECL [31]. In this path, only the co-reactant TPrA is oxidized at the electrode, and the resulting radicals, $TPrA^{\cdot+}$ and $TPrA^{\cdot}$, diffuse over short distances and react with the luminophore to generate its excited state. Maximum ECL intensity occurs in the micrometric region where concentrations of $TPrA^{\cdot+}$ and $TPrA^{\cdot}$ radicals are locally the highest. Only the luminophores located in the 3-μm region next to the electrode contribute to the ECL signal, and this finite reaction layer defines the optimal size of the functionalized beads for the bioassays [32]. This "revisited" route is essential in bead-based ECL assays and also to propose novel strategies for ECL immunosensing [109].

Many ECL-based immunoassays have been reported in the literature and are commercially available. Overall, they were first dedicated to the detection of cancer biomarkers, then for cardiovascular dysfunctions, for hormones and drugs, and for major immune antibodies such as the IgG [13]. Cancer markers detected by ECLIA include the α-fetoprotein (AFP), the carbohydrate antigen, the carcinoma

embryonic antigen, the human chorionic gonadotrophin antigen, and the prostate protein antigen. Heart dysfunctions are analyzed owing to platelet-derived growth factor, Human Cardiac Troponin I marker [110]; the human hormone glucagon [111], IgG [112], and drugs like clenbuterol [113] can be analyzed from blood samples. Extremely sensitive detections of these biomarkers have been achieved owing to the rapid developments of nanomaterials [63, 114–117] notably over the last decade, since they act (see Sect. 3.4 for detailed properties) as: (1) architectures to load large amounts of ECL labels; (2) energy acceptors to quench ECL; (3) novel labels for ECL detection; (4) electrocatalysts of ECL reactions.

Quantum dots (QDs) are increasingly used in the development of ECL bioassays. As explained above, they have appeared as very promising ECL luminophores since they offer a broad excitation spectrum, a narrow and size-tunable luminescence spectrum, a high resistivity towards photobleaching and a high-quantum yield [47–49, 118]. Most of the ECL immunoassays with QDs are based on the quenching, inhibition, or enhancement of the ECL intensities in co-reactant-depending ECL systems, using either $S_2O_8^{2-}$, SO_3^{2-}, or H_2O_2 as co-reactant [119]. Let us mention in particular the work by Peng et al. who reported the first label-free ECL immunosensor based on CdSe QDs. These were electrodeposited directly on a gold electrode from an electrolyte solution (containing cadmium sulfate, ethylenediamine tetra-acetate, and selenium dioxide) by cycling the potential between 0 and −1.2 V versus SCE [120]. The antibody was directly immobilized onto the Au electrode modified by CdSe, which had enough binding sites though being electrodeposited. The specific immunoreaction of AFP with anti-AFP resulted in the decrease of ECL intensity. Another striking result was reported by Tian et al. [121]. They showed an ECL immunoassay method for ultrasensitive detection of prostate protein antigen, by remarkably efficient energy-transfer-induced ECL quenching from the CdS QDs sensitized TiO_2 nanotube array to the activated CdTe QDs functionalized multi-walled carbon nanotubes (MWCNTs) composite. The ECL intensity decrement was logarithmically related to the concentration of the prostate protein antigen (PSA) in the range of 1.0 fg mL^{-1} to 10 pg mL^{-1} with a LOD of 1 fg mL^{-1}. Using CdSe QDs as ECL emitters, Ju et al. were able to monitor the carbohydrate expression on living cells by combining the specific recognition of lectin to carbohydrate groups with the functionalization of immobilized QDs [122].

However, it must be pointed out that the limited functionalization of ligands and variable efficiency in the bioconjugation to antibodies are the main drawbacks of QDs. Several approaches are proposed for the conjugation of QDs with Ab2: (1) the direct conjugation of amino/carboxyl groups using actived esters; (2) a direct conjugation to the QDs surface through the antibody thiol groups; (3) indirect conjugations using bridge proteins such as a modified protein G or avidin reacting with biotinylated antibodies. Ultimately, any employed QDs should be previously modified in order to obtain water solubility and the required functional groups, preferably carboxylate or amino groups.

Noble metal particles structured at the nanoscale are also favorable NPs for ECL with improved mass transport and electron conductivity [5, 58, 115, 123–125]. For instance, nanoporous gold has attracted considerable attention in recent years due to its high surface-to-volume ratio, high in-plane conductivity, good stability, and biocompatibility. These nanoporous materials have been used for electrochemical sensors, while they are basically used as ECL labels [126]. The primary antibody was immobilized on the Au NPs modified electrode through L-cysteine and glutaraldehyde, and then the antigen and the functionalized ruthenium-modified silica nanoporous gold composite-labeled secondary antibody were conjugated successively to form a sandwich-type immunocomplex through the specific interaction. Nanoporous Pt–Ru alloy has also been widely studied because of its uniform structural dimensions [102, 126].

Besides, nanosized-carbon particles, materials, and nanoelectrodes constitute a very promising category [109, 115, 123, 127, 128]. Especially, graphene sheets, with their two-dimensional structure, unique mechanical properties, excellent conductivity, large surface area, unique graphitized basal plane structure, as well as good biocompatibility might be excellent supporting material for signal amplification in ECL sensors. Chitosan-functionalized graphene-modified glassy-carbon electrodes have been employed to increase the loading of Ab1 and catalyzed the cathodic ECL reaction, which was further amplified by gold nanorods and an enzyme-catalyzed reaction [129]. Another striking example is an ECL immunosensor prepared from graphene-CdS QDs-alginate as the immobilizing support and CdSe/ZnS QDs as the label. CdSe/ZnS QDs labeled on the Ab2 could absorb emitted photons in the system, providing a possible application in bioassays of QDs [121]. In parallel, CNTs are attractive as building blocks for ECL sensors because they possess a unique combination of excellent electrical and electrochemical properties, they can be easily modified with different functional groups for the attachment of biomolecules [130, 131], and they possess a very high surface-area-to-weight ratio. Paolucci et al. exploited these remarkable properties of CNTs to build a highly sensitive ECL biosensor for the detection of palytoxin, a potent marine toxin which contaminates seafood [132]. They obtained very reproducible and reliable responses in complex matrices, such as mussels and microalgae, reaching the LOD of 0.07 ng mL^{-1}. Recently, an interfusion of graphene and CNT in a Nafion film was coated on an electrode for $Ru(bpy)_3^{2+}$ adsorption in order to demonstrate the co-reactant-based approach of the $Ru(bpy)_3^{2+}$/poly(ethylenimine) system for human chorionic gonadotrophin ECLIA [104].

All these different strategies based on ever more and more complex architectures lead currently to exceptionally sensitive ECLIA. They are all solely based on the high specificity of the antigen–antibody interaction. However, diagnostic applications would ultimately require the simultaneous analysis of several antibodies from the same sample (especially in the blood). This task should be performed using either multilabel, or multianalyte (on an array) strategies [106, 133, 134], both

constituting specific research areas dedicated to the analytical methodology [135–139].

4.2 DNA Assays

DNA is the second main biological target of ECL bioassays. Indeed, the sensitive detection of DNA is of great importance for medical diagnosis, environmental investigations, gene expression analysis, pharmaceutical studies, forensic analyses, etc. [140, 141]. ECL DNA assays include mainly two types of label-free and label-based ECL detection strategies. Meanwhile, various amplification techniques have been used to improve the sensitivity of DNA detection [43, 142, 143]. These include nanomaterials with multiple grafting sites to increase the number of tags, enzyme-assisted signal-amplification processes, and DNA-amplification techniques such as rolling-circle amplification (RCA), target-induced repeated primer extension, hybridization chain reaction (HCR), and loop-mediated amplification [144].

First, metal or semiconductor NPs, owing to their unique optical and electrical properties, were widely employed as labels for the amplified detection of DNA. Since a single NP (e.g., Au NP) can be loaded with thousands of DNA molecules, the ECL intensity is typically enhanced by 2–3 orders of magnitude on an Au NP self-assembled electrode compared with a bare gold electrode. Jiang et al. developed a novel ECL DNA sensor for *Mycobacterium tuberculosis* (MTB), by using luminol-functionalized Au NPs [124, 125] as labels [145]. Owing to these novel ECL labels, the amplification by Au NPs and the biotin–streptavidin system, extremely high sensitivity (LOD of 170 pg L^{-1}) for a single-stranded DNA (ssDNA) was obtained.

Then, among the techniques for DNA amplification, RCA is a powerful, though simple, biochemical method based on the use of a DNA polymerase to generate long, linear, tandem, repetitive, ssDNA under isothermal conditions (Fig. 8). As the synthesized long DNA molecules contain many repetitive sequence motifs, this improves the biosensor analytical properties. For instance, Jiang et al. reported a highly sensitive strategy for the ECL detection of DNA of *Clostridium perfringens* [146]. In the presence of target DNA, the RCA primer was attached to the electrode and the RCA reaction was executed isothermally. The products of RCA were incubated with hemin to form hemin/G-quadruplex DNAzymes, which competitively consumed oxygen in the detection buffer and thus quenched the ECL emission of the $O_2/S_2O_8^{2}$ system. The decrease of ECL emission was related to the quantity of the target DNA, so that the ECL sensor provided both sensitivity to detect the amount of *Clostridium perfringens* target DNA, and also the selectivity to discriminate target DNA from non-target sequences even with a difference of only one base.

DNA nanoassembly via target-probe hybridization is a simple and effective approach to build ECL DNA sensors. If properly designed, DNA can assemble into

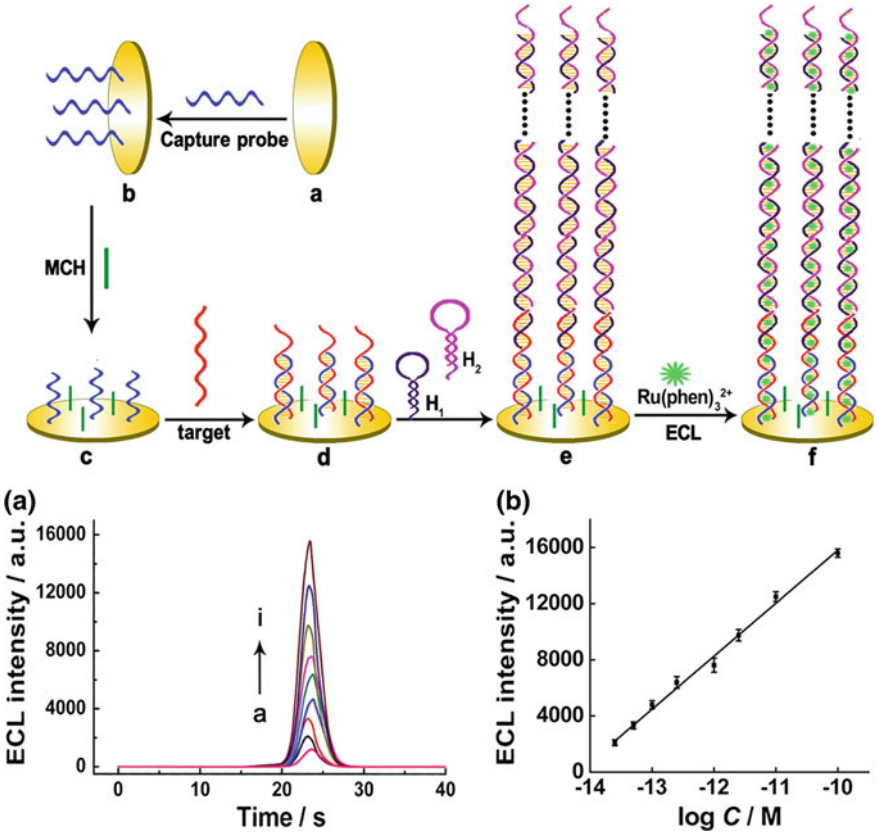

Fig. 8 ECL detection of DNA based on a HCR strategy. *Top* ECL measurements are obtained after immobilizing the capture DNA, adding 2.5 pM of target DNA and making hairpin probes reacting with the hybridized system. Subsequently, 2 mM $Ru(phen)_3^{2+}$ is added so as to intercalate with the DNA assembly and provide ECL in 0.1 M phosphate buffer solution (pH 7.5) containing 20 mM TPrA. *Below* **a** ECL responses of the sensor to different concentrations of target DNA (*a*) 0 fM, (*b*) 25 fM, (*c*) 50 fM, (*d*) 100 fM, (*e*) 250 fM, (*f*) 1 pM, (*g*) 2.5 pM, (*h*) 10 pM, (*i*) 100 pM. **b** The resulting calibration plot of log c versus ECL intensity [147]. Reprinted with permission from Ref. [147]. Copyright 2012 American Chemical Society

different structures in two- or three dimensions. Based on long-range, self-assembled, DNA nanostructures as carriers for ECL signal amplification, Liu et al. fabricated a label-free, ultrasensitive ECL biosensor for detection of microRNA-21, a biomarker for cancers and other diseases (Fig. 9) [148]. Due to the high sensitivity (1 fM LOD) and high selectivity, wide linear range (1 fM–1 pM) and simplicity of the methodology, this approach is of particular interest.

HCR is another DNA-nanoassembly method for DNA detection; this is an enzyme-free process, where a hybridization event is triggered by an initiator (target) and leads to the polymerization of oligonucleotides into a long nicked

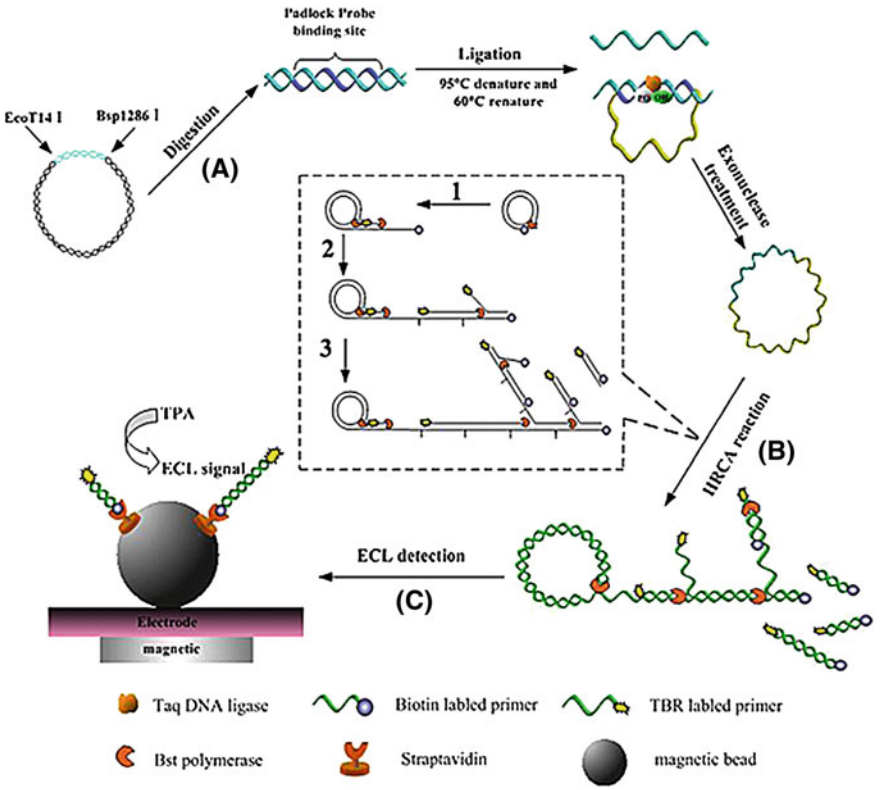

Fig. 9 Principle of magnetic bead-based ECL hyperbranching rolling circle amplification (HRCA) assay for DNA (from Listeria monocytogenes herein). (A) Genomic DNA digestion and padlock-probe circularization. (B) HRCA reaction with a biotin-labeled primer and a $Ru(bpy)_3^{2+}$-labeled primer. (C) ECL detection [148]. Reprinted with permission of Springer from Ref. [148]

double-stranded DNA (dsDNA). The HCR-based ECL strategy not only enables low femtomolar detection of sequence-specific DNA, but also shows high selectivity against single-base mismatch sequences. As an example, a highly sensitive, universal strategy for ECL detection of a DNA sequence specific to *Escherichia coli* was reported based on a HCR amplification approach [147]. Authors obtained a linear response between 25 fM and 100 pM with an estimated LOD of 15 fM for a DNA sequence, which is a copy of partial region of the *E. coli* 16S rRNA gene, specific to urinary tract infections.

Besides, ECL starts to be used to assess DNA damages, which include the oxidation, alkylation, or hydrolysis of bases, adducts' formation, and mismatch of bases caused by environmental hazards. Many biological methods such as the comet assay and the unscheduled DNA-synthesis test have been used to detect DNA damages. However, these methods are complex, time consuming, and have

low efficiency and sensitivity. Recently was reported an ECL biosensor to detect specific sequences of DNA by using CdTe@SiO_2 as nanoprobes for signal amplification [149, 150]. Based on the ECL detection of CdTe@SiO_2 labeled on probe DNA, a sensitive assay for the sequence-specific DNA detection was developed. The "sandwich-type" DNA complexes were fabricated by self-assembly of an aminated capture DNA on a glassy-carbon electrode and hybridized with one end of target DNA, the other end of which was recognized with signal DNA labeled with CdTe@SiO_2. Under optimum conditions, the peak current value increased with the concentration of target DNA within a wide dynamic range (0.1 nM–2 μM) and an excellent LOD (30 pM). An ECL signal corresponding to a single-base-mismatch was also detected. The experiments indicated that the sensing system could differentiate single-base-mismatched DNA from complementary DNA. Strikingly, the biosensor could successfully be applied to study the DNA damage induced by several genotoxic chemicals (styrene, aflatoxin, ochratoxin, methanol, and ethanol) [150].

In recent years, isothermal amplification reactions based on DNA machines attracted much attention in designing sensitive analysis of DNA and single-nucleotide polymorphism (SNP) for their autonomous circular amplification and simple operations [151]. These isothermal amplification reactions use enzyme-assisted replication or scission reactions as the DNA machines. A new ECL approach for detection of SNPs was based on an isothermal cycle-assisted, triple-stem probe labeled with gold and CdTe NPs [152]. With its simplicity, selectivity, and sensitivity, this molecular tool holds great promise for SNP discovery and analysis, and might be extensively applied in the future for clinical research and diagnostics.

As already mentioned, the detection of DNA damages by oxidative stress processes or by chemicals is also a central biomedical issue. Rusling et al. demonstrated in a series of articles that ECL can be obtained in ultrathin metallopolymer films containing either osmium or ruthenium complexes from oxidized DNA without using a sacrificial co-reactant [133, 134, 153]. The guanine bases present in oligonucleotides generate the ECL emission by reacting with the organometallic complexes. ECL signals are sensitive to oligonucleotide hybridization and chemical damage of dsDNA [153]. Such an approach allowed them to detect DNA oxidation and nucleobase adducts from chemical damage, such as 8-oxoguanine [133]. ECL arrays were thus reported to screen the relative propensity of different enzymes (e.g., cytochrome P450 enzymes) to produce genotoxic metabolites [134].

4.3 Aptamers ECL Sensors

A large number of functional oligonucleotides including aptamers and DNAzymes have been synthesized and used for the development of biosensors [154, 155]. Consequently, they have attracted increasing interest recently for ECL bioanalytical applications. Aptamers are single-stranded nucleic acids (DNA or RNA) with

special structures that allow high recognition ability to a broad range of molecular targets including small molecules, ions, proteins, and even whole cells. Aptamers exhibit many advantages when compared to traditional molecular recognition elements, including simple synthesis, good stability, easy storage, high affinity and specificity, and possible further chemical modifications for their processing.

Various protocols of aptamer-based ECL biosensing for the determination of proteins and small molecules have been reported [156, 157]. A striking example for the ultrasensitive ECL detection of thrombin was reported by Chen et al. [158]. The sensor is based on layer-by-layer assembly of CdTe QDs onto polystyrene microbeads as ECL signal amplification labels (Fig. 10). Upon using these polystyrene-$(CdTe)_2$ labels, and playing with the number of QD layers, about 2–4 orders of magnitude improvement in the LOD for thrombin (350 fM) was obtained when compared with other signal amplification routes. ECL aptasensors for the detection of small molecules have also been widely reported. ECL quenching of $Ru(bpy)_3^{2+}$-labeled silica NPs by ferrocene was used to analyze adenosine [159]. First, complementary DNA strands, labeled with the $Ru(bpy)_3^{2+}$-silica NPs, were immobilized onto the gold electrode. Then, ferrocene-labeled aptamer was provided to hybridize the complementary DNA on the electrode surface, resulting in the quenching of ECL from $Ru(bpy)_3^{2+}$. In the presence of adenosine, the ferrocene-labeled aptamer preferentially forms an adenosine–aptamer complex and prevents DNA hybridization, which induces an ECL signal recovery. By using this approach, a LOD of 31 pM for adenosine was achieved.

Though being extremely efficient and sensitive, the above approaches involve complicated modification procedures. Thus, label-free ECL detection is also extensively investigated according to its advantages of simplicity. In particular, label-free and sensitive ECL aptasensors for cations were developed. In a first example, dedicated to the detection of potassium ions, Dang et al. have reported that a free-state G-rich DNA aptamer can enhance the ECL signal of chitosan/$Ru(bpy)_3^{2+}$/silica NPs on an electrode more effectively than its G-quadruplex structure which binds K^+ [160]. By analyzing the decrease of ECL signal, a LOD of 300 pM for K^+ was achieved. ECL probe intercalation in DNA aptamers was used for a label-free and "turn-on" sandwich ECL biosensor for Hg^{2+} ions; this was based on the thymidine–Hg^{2+}–thymidine coordination [161]. In this protocol, two functional ssDNA were designed with a thymidine-rich section for the recognition of mercury ions and could partially hybridize with each other forming an intermolecular duplex for the intercalation of $Ru(phen)_3^{2+}$ luminophore. Owing to the specificity of interaction between Hg^{2+} and multithymidine, and high sensitivity of super sandwich ECL detection, a LOD of 250 pM for mercury was obtained.

Besides small molecules and proteins, ECL aptasensors have also been used for the detection of cell markers [92, 162, 163]. An ultrasensitive hybrid bipolar electrode–ECL biosensor for the detection of cancer cell surface proteins was recently proposed [162] by using a ferrocene-labeled aptamer as a signal recognition and amplification probe. The hybrid bipolar electrode (see part 3.5 for details on ECL in bipolar electrochemistry) is composed of an ITO-coated glass as the anode, and Au NPs as the

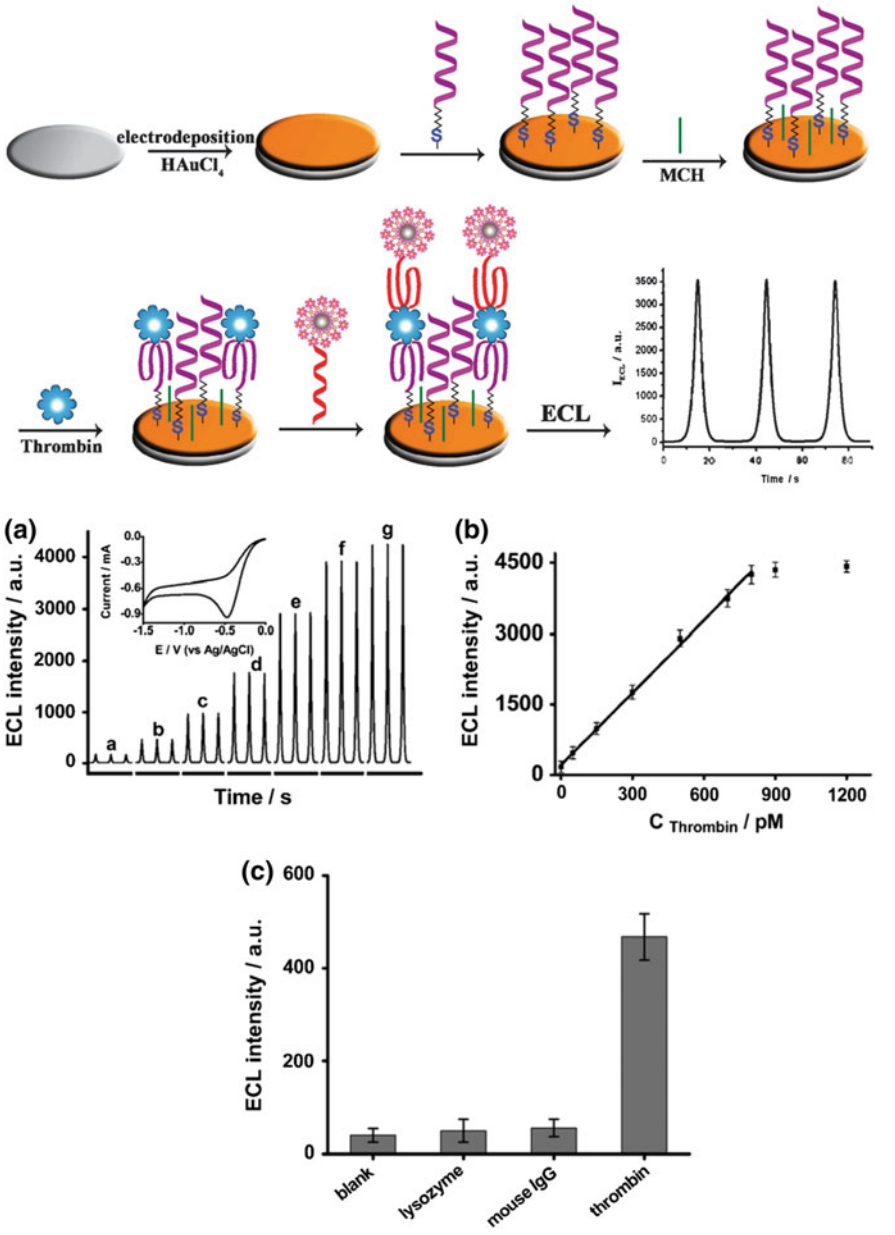

cathode. Owing to its conductivity and large surface area, this system provides large cathodic currents resulting in enhanced ECL of the $Ru(bpy)_3^{2+}$–TPrA system on the anode. Then, a ferrocene-labeled aptamer was introduced to hybridize the capture DNA immobilized on the cathode NPs. Ferrocene quenched the ECL response,

◀ **Fig. 10** *Top* Schematic of the different steps for the construction of an ECL sensor for thrombin. It consists in the deposition of gold nanoparticles (Au NPs) on a glassy-carbon electrode, the self-assembly of the primary thrombin-binding aptamer on the Au NP-modified electrode, the surface blocking with 6-mercapto-1-hexamine (MCH), the association of the thrombin analyte with the primary thrombin-binding aptamer and the secondary thrombin binding aptamer-conjugated PS bead-$(CdTe)_2$ QDs. *Down* **a** ECL profiles for thrombin detection based on PS-$(CdTe)_2$ assembly label at different concentrations: (*a*) 0.5 pM, (*b*) 50 pM, (*c*) 150 pM, (*d*) 300 pM, (*e*) 500 pM, (*f*) 700 pM and (*g*) 800 pM. *Inset* Typical voltammogram corresponding to the presence of 500 pM thrombin. **b** Calibration plot of ECL intensity versus thrombin concentration. **c** Selectivity of the ECL detection of thrombin (50 pM) against interference proteins, including lysozyme (500 pM) and mouse IgG (500 pM) [158]. Reprinted with permission from Ref. [158]. Published by The Royal Society of Chemistry

which can recover in the presence of cancer cells, since labeled aptamers can combine with target proteins expressed on the cell surface. The coupling of the cathodic ECL at Au nanoparticles with the anodic ferrocene induced signal quenching amplification, allowed a LOD of 20 cells with this approach.

4.4 Enzymatic Assays

Also for the detection of enzymatic reactions, ECL has some distinct advantages because the, in many cases highly selective, enzymatic activity can be tracked in time and space if at least one of the reaction products can act as a co-reactant in one or the other of the classic ECL systems. Depending on which compound is produced by the enzyme, there are mainly three options that have been largely explored and also extensively reviewed in the recent literature [4, 41, 164].

The first very common possibility is to use enzymes belonging to the family of dehydrogenases. The "by-product" of their enzymatic activity is the transformation of the coenzyme NAD^+ into NADH. The latter one can play the role of an ECL co-reactant for the $Ru(bpy)_3^{2+}$ system because, exactly like TPrA, it has a tertiary amine function. Therefore, and under the condition that $Ru(bpy)_3^{2+}$ is present in excess, the recorded ECL signal is directly proportional to the production of reduced coenzyme, which in turn is correlated with the concentration of the enzyme's substrate in solution. The family of dehydrogenases contains hundreds of enzymes belonging to the group of oxidoreductases which oxidize a substrate and transfer one or more hydrides to an electron acceptor such as NAD^+. Therefore, this gives access to ECL analysis of classic analytes such as glucose [165] or ethanol [166], but in principle also many other biologically relevant substrates can be detected based on this concept.

A second approach is based on the fact that another family of oxidoreductases, namely oxidases uses oxygen as an electron acceptor instead of NAD^+, and therefore produces hydrogen peroxide as a side product. This obviously allows working with the luminol/H_2O_2 ECL system as an optical readout of the enzymatic

activity, again either for the most frequent analytes like glucose [167], but also for analytes which were not accessible with the $Ru(bpy)_3^{2+}$/NAD^+ system [168–170].

The third possibility which has been widely studied to couple an enzymatic reaction with an ECL producing system involves the use of quantum dots. ECL with QDs has been investigated, among others, for co-reactants which can be correlated with enzymatic activity (e.g., H_2O_2, O_2). Cathodic and anodic ECL processes have been explored in this context. For cathodic ECL, QDs and H_2O_2 are simultaneously reduced at the electrode, and then the produced hydroxyl radical can act as a strong oxidizing agent and inject a hole into the QD, which can further react to generate an excited state by annihilation. In this way, most enzymes producing H_2O_2 are in principle able to enhance QD ECL [171]. It is also possible to develop enzymatic ECL biosensors utilizing anodic QD ECL [172]. However, a drawback can be in some cases the quite high positive potentials which are necessary to trigger the process.

These listed reaction schemes are usually carried out in conventional three-electrode electrochemical setups, but as already mentioned in Sect. 3.5, one quite original and promising extension of these approaches is to trigger ECL in a bipolar electrochemistry configuration. Recently, a couple of enzymatic systems were employed for analyte detection based on bipolar electrochemistry. Oxidation of blood glucose by means of glucose oxidase yielding H_2O_2 was analyzed in a three-compartment closed bipolar sensing platform allowing a straightforward wireless readout of the chemical information based on $Ru(bpy)_3^{2+}$ ECL [85]. The luminol system has also been explored in a bipolar configuration for detecting glucose [87]. In this case, the H_2O_2 generated by the enzymatic reaction was not directly involved in the ECL generation as a co-reactant, but was reduced at the bipolar cathode with the help of a catalytically active Prussian Blue layer (Fig. 11a). This reduction reaction was intrinsically coupled with the luminol/H_2O_2 oxidation at the anodic side of the bipolar electrode, leading finally to a light signal which is proportional to the glucose concentration. Very recently, it has been possible to extend this approach to a dual enzymatic detection [173] based on the concept of 3D ECL described in Sect. 3.5 [97, 98].

Another interesting extension based on the synergistic combination of enzymatic ECL detection with bipolar electrochemistry is based on the fact that the latter one can also be used in a very simple way to generate motion [174, 175]. If such a motion is coupled with ECL emission, this leads to a light-emitting moving object [95]. If in addition the ECL reaction is triggered by an enzymatic step, this results in a roving biosensor [99]. As a consequence, this gives access to spatio-temporal detection of varying concentrations of an analyte based on the light emission from a single object cruising through the solution (Fig. 11b).

Although these last examples are for the moment at the stage of academic research, it can be envisioned that such new concepts might help in the future to map enzymatically the analyte concentration in inhomogeneous samples either by 3D ECL or by the roving single particle approach. Naturally, all the studies mentioned in this paragraph can also be extended towards the elaboration of

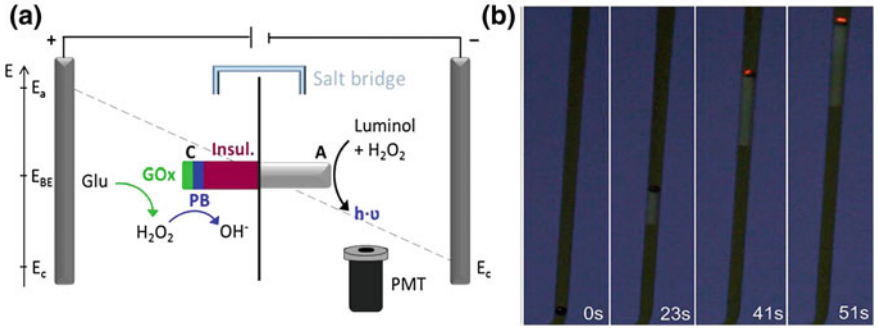

Fig. 11 **a** Schematic illustration of the measurement concept for the bipolar enzymatic ECL detection of glucose with the luminol/H_2O_2 system [87]. **b** Enzymatic ECL sensing of glucose concentration with a moving particle. Series of optical images showing a GC bead emitting ECL at different times during its motion. The bead is positioned in a capillary filled with 100 mM PBS solution (pH = 7.4) containing 9.28 U mL^{-1} GDH, 1.5 mM $Ru(bpy)_3^{2+}$, 10 mM NAD^+ and a few drops of surfactant. When it reaches a glucose-rich region, while moving towards the top of the capillary, light emission starts [99]. Reprinted with permission of Elsevier from Ref. [87]. Reprinted with permission from Ref. [99]. Published by The Royal Society of Chemistry

immunosensors and DNA sensing, as enzymes can be easily used as labels in these kinds of systems (see Sects. 4.1 and 4.2). This again underlines the tremendous application potential of these concepts.

5 Conclusion and Perspectives

Since the first reports in the 1960s, ECL has evolved from an interesting laboratory phenomenon to a powerful ultrasensitive analytical technique. It is a very versatile method because it combines the principles and the tools of both electrochemistry and photochemistry. Therefore, more factors are involved in the global ECL process which expands the interplay possibilities. In addition to the developments in its own area, progresses in each of these fields may also lead to advances in the ECL domain. Its remarkable characteristics and the discovery of co-reactant ECL in aqueous solutions make such readout mechanisms particularly attractive for bioanalytical applications. Thus, ECL is currently commercialized in the clinical diagnostic market for a wide range of immunoassays measuring specific biomarkers involved in different pathologies, such as cardiac and infectious diseases, thyroid disorders, and tumors.

Looking to the future, it seems obvious that ECL will find more analytical applications due to the demand in medical diagnostics for lower LODs, in biodefense, and in environmental analysis. However, fundamental research on ECL remains also essential for continuing to push the barriers which we believed to be unsurpassable at a given time, as usual in science. For example, compared to

chemiluminescence, one of the main restrictions of ECL is the confinement of the process to the electrode surface. To overcome such a limitation, 3D bulk ECL has been generated at the level of millions of micro- and nano-emitters dispersed in solution [97]. Addressing the electrodes in a wireless manner by bipolar electrochemistry gave thus various original applications [78, 83]. Another area that is expected to grow rapidly is the paper-based microfluidic sensors based on ECL detection and portable multiplexed systems with a high degree of integration [84, 176, 177]. The research on new efficient co-reactants [27], of luminophores emitting at different wavelengths [177–181] and of new nano-objects (e.g., Au NPs [58–60], QDs [48, 49], and doped silica NPs [182, 183]), offers the opportunity to develop new analytical detection strategies and assays, but also to continue to study fundamental issues in chemistry, biology or physics.

References

1. Bard, A.J., Faulkner, L.R.: Electrochemical Methods: Fundamentals and Applications, 2nd edn. Wiley, New York (2001)
2. Bard, A.J.: Electrogenerated Chemiluminescence. M. Dekker, New York (2004)
3. Kapturkiewicz, A.: In: Alkire, R.C., Gerischer, H., Kolb, D.M., Tobias, C.W. (eds.): Advances in Electrochemical Science and Engineering, vol. 5, p. 1. Wiley-VCH
4. Miao, W.: Chem. Rev. **108**, 2506 (2008)
5. Bertoncello, P., Stewart, A.J., Dennany, L.: Anal. Bioanal. Chem. **406**, 5573 (2014)
6. Forster, R.J., Bertoncello, P., Keyes, T.E.: Ann. Rev. Anal. Chem. **2**, 359 (2009)
7. Richter, M.M.: Chem. Rev. **104**, 3003 (2004)
8. Rampazzo, E., Bonacchi, S., Genovese, D., Juris, R., Marcaccio, M., Montalti, M., Paolucci, F., Sgarzi, M., Valenti, G., Zaccheroni, N., Prodi, L.: Coord. Chem. Rev. **256**, 1664 (2012)
9. Liu, Z., Qi, W., Xu, G.: Chem. Soc. Rev. **44**, 3117 (2015)
10. Yang, H., Leland, J.K., Yost, D., Massey, R.J.: Nat. Biotechnol. **12**, 193 (1994)
11. Blackburn, G.F., Shah, H.P., Kenten, J.H., Leland, J., Kamin, R.A., Link, J., Peterman, J., Powell, M.J., Shah, A., Talley, D.B., Tyagi, S.K., Wilkins, E., Wu, T.G., Massey, R.J.: Clin. Chem. **37**, 1534 (1991)
12. Zhou, X., Zhu, D., Liao, Y., Liu, W., Liu, H., Ma, Z., Xing, D.: Nat. Protoc. **9**, 1146 (2014)
13. Muzyka, K.: Biosens. Bioelectron. **54**, 393 (2014)
14. Yuan, Y., Han, S., Hu, L., Parveen, S., Xu, G.: Electrochim. Acta **82**, 484 (2012)
15. Ege, D., Becker, W.G., Bard, A.: J. Anal. Chem. **56**, 2413 (1984)
16. Hercules, D.M.: Science **145**, 808 (1964)
17. Visco, R.E., Chandross, E.A.: J. Am. Chem. Soc. **86**, 5350 (1964)
18. Santhanam, K.S.V., Bard, A.J.: J. Am. Chem. Soc. **87**, 139 (1965)
19. Tokel-Takvoryan, N.E., Hemingway, R.E., Bard, A.J.: J. Am. Chem. Soc. **95**, 6582 (1973)
20. Tokel, N.E., Bard, A.J.: J. Am. Chem. Soc. **94**, 2862 (1972)
21. Rubinstein, I., Bard, A.J.: J. Am. Chem. Soc. **103**, 512 (1981)
22. Noffsinger, J.B., Danielson, N.D.: Anal. Chem. **59**, 865 (1987)
23. Leland, J.K., Powell, M.J.: J. Electrochem. Soc. **137**, 3127 (1990)
24. Bard, A.J., Whitesides, G.M.: US Patent 5,221,605, 22 June 1993
25. Faulkner, L.R., Bard, A.J.: J. Am. Chem. Soc. **90**, 6284 (1968)
26. Glass, R.S., Faulkner, L.R.: J. Phys. Chem. **85**, 1160 (1981)
27. Liu, X., Shi, L., Niu, W., Li, H., Xu, G.: Angew. Chem. Int. Ed. **46**, 421 (2007)
28. Zu, Y., Bard, A.: J. Anal. Chem. **73**, 3960 (2001)

29. Kanoufi, F., Zu, Y., Bard, A.J.: J. Phys. Chem. B **105**, 210 (2001)
30. Zu, Y., Bard, A.: J. Anal. Chem. **72**, 3223 (2000)
31. Miao, W., Choi, J.-P., Bard, A.J.: J. Am. Chem. Soc. **124**, 14478 (2002)
32. Sentic, M., Milutinovic, M., Kanoufi, F., Manojlovic, D., Arbault, S., Sojic, N.: Chem. Sci. **5**, 2568 (2014)
33. Cruser, S.A., Bard, A.J.: Anal. Lett. **1**, 11 (1967)
34. Rubinstein, I., Martin, C.R., Bard, A.: J. Anal. Chem. **55**, 1580 (1983)
35. Skotty, D.R., Nieman, T.A.J.: Chromatogr. B: Biomed. Sci. Appl. **665**, 27 (1995)
36. Yamashita, K., Yamazaki-Nishida, S., Harima, Y., Segawa, A.: Anal. Chem. **63**, 872 (1991)
37. Knight, A.W., Greenway, G.M.: Analyst **120**, 2543 (1995)
38. Knight, A.W., Greenway, G.M.: Analyst **121**, 101R (1996)
39. Downey, T.M., Nieman, T.A.: Anal. Chem. **64**, 261 (1992)
40. Brune, S.N., Bobbitt, D.R.: Anal. Chem. **64**, 166 (1992)
41. Chen, X.-M., Su, B.-Y., Song, X.-H., Chen, Q.-A., Chen, X., Wang, X.-R.: Trac-Trend Anal. Chem. **30**, 665 (2011)
42. Kenten, J.H., Casadei, J., Link, J., Lupold, S., Willey, J., Powell, M., Rees, A., Massey, R.: Clin. Chem. **37**, 1626 (1991)
43. Miao, W., Bard, A.: J. Anal. Chem. **75**, 5825 (2003)
44. Zhang, J., Qi, H., Li, Y., Yang, J., Gao, Q., Zhang, C.: Anal. Chem. **80**, 2888 (2008)
45. Li, Y., Qi, H., Peng, Y., Yang, J., Zhang, C.: Electrochem. Commun. **9**, 2571 (2007)
46. Wu, P., Hou, X., Xu, J.-J., Chen, H.-Y.: Chem. Rev. **114**, 11027 (2014)
47. Zhao, W.-W., Wang, J., Zhu, Y.-C., Xu, J.-J., Chen, H.-Y.: Anal. Chem. **87**, 9520 (2015)
48. Ding, Z., Quinn, B.M., Haram, S.K., Pell, L.E., Korgel, B.A., Bard, A.J.: Science **296**, 1293 (2002)
49. Myung, N., Ding, Z., Bard, A.J.: Nano Lett. **2**, 1315 (2002)
50. Zou, G., Ju, H.: Anal. Chem. **76**, 6871 (2004)
51. Myung, N., Bae, Y., Bard, A.J.: Nano Lett. **2003**, 3 (1053)
52. Bae, Y., Myung, N., Bard, A.J.: Nano Lett. **4**, 1153 (2004)
53. Jie, G., Liu, B., Pan, H., Zhu, J.-J., Chen, H.-Y.: Anal. Chem. **79**, 5574 (2007)
54. Liu, X., Jiang, H., Lei, J., Ju, H.: Anal. Chem. **79**, 8055 (2007)
55. Zheng, L., Chi, Y., Dong, Y., Lin, J., Wang, B.: J. Am. Chem. Soc. **131**, 4564 (2009)
56. Zhu, H., Wang, X., Li, Y., Wang, Z., Yang, F., Yang, X.: Chem. Commun. **5118** (2009)
57. Li, L.-L., Ji, J., Fei, R., Wang, C.-Z., Lu, Q., Zhang, J.-R., Jiang, L.-P., Zhu, J.-J.: Adv. Funct. Mater. **22**, 2971 (2012)
58. Swanick, K.N., Hesari, M., Workentin, M.S., Ding, Z.: J. Am. Chem. Soc. **134**, 15205 (2012)
59. Hesari, M., Workentin, M.S., Ding, Z.: Chem. Sci. **5**, 3814 (2014)
60. Hesari, M., Workentin, M.S., Ding, Z.: ACS Nano **8**, 8543 (2014)
61. Li, L., Liu, H., Shen, Y., Zhang, J., Zhu, J.-J.: Anal. Chem. **83**, 661 (2011)
62. Diez, I., Pusa, M., Kulmala, S., Jiang, H., Walther, A., Goldmann, A.S., Mueller, A.H.E., Ikkala, O., Ras, R.H.A.: Angew. Chem. Int. Ed. **48**, 2122 (2009)
63. Bertoncello, P., Forster, R.J.: Biosens. Bioelectron. **24**, 3191 (2009)
64. Obeng, Y.S., Bard, A.J.: Langmuir **7**, 195 (1991)
65. Rubinstein, I., Bard, A.J.: J. Am. Chem. Soc. **102**, 6641 (1980)
66. Khramov, A.N., Collinson, M.M.: Anal. Chem. **72**, 2943 (2000)
67. Choi, H.N., Cho, S.-H., Lee, W.-Y.: Anal. Chem. **75**, 4250 (2003)
68. Guo, Z., Shen, Y., Wang, M., Zhao, F., Dong, S.: Anal. Chem. **76**, 184 (2004)
69. Zhang, L., Dong, S.: Anal. Chem. **78**, 5119 (2006)
70. Jie, G., Zhang, J., Wang, D., Cheng, C., Chen, H.-Y., Zhu, J.-J.: Anal. Chem. **80**, 4033 (2008)
71. Wang, J., Shan, Y., Zhao, W.-W., Xu, J.-J., Chen, H.-Y.: Anal. Chem. **83**, 4004 (2011)
72. Wang, Y., Lu, J., Tang, L., Chang, H., Li, J.: Anal. Chem. **81**, 9710 (2009)
73. Li, L.-L., Liu, K.-P., Yang, G.-H., Wang, C.-M., Zhang, J.-R., Zhu, J.-J.: Adv. Funct. Mater. **21**, 869 (2011)

74. Xu, S., Liu, Y., Wang, T., Li, J.: Anal. Chem. **83**, 3817 (2011)
75. Zhang, J., Gryczynski, Z., Lakowicz, J.R.: Chem. Phys. Lett. **393**, 483 (2004)
76. Yuk, J.S., O'Reilly, E., Forster, R.J., MacCraith, B.D., McDonagh, C.: Chem. Phys. Lett. **513**, 112 (2011)
77. Devadoss, A., Dickinson, C., Keyes, T.E., Forster, R.: J. Anal. Chem. **83**, 2383 (2011)
78. Fosdick, S.E., Knust, K.N., Scida, K., Crooks, R.M.: Angew. Chem. Int. Ed. **52**, 10438 (2013)
79. Loget, G., Zigah, D., Bouffier, L., Sojic, N., Kuhn, A.: Acc. Chem. Res. **46**, 2513 (2013)
80. Arora, A., Eijkel, J.C.T., Morf, W.E., Manz, A.: Anal. Chem. **73**, 3282 (2001)
81. Chow, K.-F., Mavré, F., Crooks, R.M.: J. Am. Chem. Soc. **130**, 7544 (2008)
82. Chow, K.-F., Mavré, F., Crooks, J.A., Chang, B.-Y., Crooks, R.M.: J. Am. Chem. Soc. **131**, 8364 (2009)
83. Qi, W., Lai, J., Gao, W., Li, S., Hanif, S., Xu, G.: Anal. Chem. **86**, 8927 (2014)
84. Feng, Q.-M., Pan, J.-B., Zhang, H.-R., Xu, J.-J., Chen, H.-Y.: Chem. Commun. **50**, 10949 (2014)
85. Zhang, X., Li, J., Jia, X., Li, D., Wang, E.: Anal. Chem. **86**, 5595 (2014)
86. Zhang, J.-D., Yu, T., Li, J.-Y., Xu, J.-J., Chen, H.-Y.: Electrochem. Commun. **49**, 75 (2014)
87. Eßmann, V., Jambrec, D., Kuhn, A., Schuhmann, W.: Electrochem. Commun. **50**, 77 (2015)
88. Wu, S.Z., Zhou, Z.Y., Xu, L.R., Su, B., Fang, Q.: Biosens. Bioelectron. **53**, 148 (2014)
89. Shi, H.W., Wu, M.S., Du, Y., Xu, J.J., Chen, H.Y.: Biosens. Bioelectron. **55**, 459 (2014)
90. Wu, M.-S., Yuan, D.-J., Xu, J.-J., Chen, H.-Y.: Chem. Sci. **4**, 1182 (2013)
91. Zhang, X., Chen, C., Li, J., Zhang, L., Wang, E.: Anal. Chem. **85**, 5335 (2013)
92. Wu, M.-S., Yuan, D.-J., Xu, J.-J., Chen, H.-Y.: Anal. Chem. **85**, 11960 (2013)
93. Wu, M.-S., Xu, B.-Y., Shi, H.-W., Xu, J.-J., Chen, H.-Y.: Lab Chip **11**, 2720 (2011)
94. Wu, M.-S., Qian, G.-S., Xu, J.-J., Chen, H.-Y.: Anal. Chem. **84**, 5407 (2012)
95. Sentic, M., Loget, G., Manojlovic, D., Kuhn, A., Sojic, N.: Angew. Chem. Int. Ed. **51**, 11284 (2012)
96. Bouffier, L., Zigah, D., Adam, C., Sentic, M., Fattah, Z., Manojlovic, D., Kuhn, A., Sojic, N.: ChemElectroChem **1**, 95 (2014)
97. Sentic, M., Arbault, S., Bouffier, L., Manojlovic, D., Kuhn, A., Sojic, N.: Chem. Sci. **6**, 4433 (2015)
98. de Poulpiquet, A., Diez-Buitrago, B., Milutinovic, M., Goudeau, B., Bouffier, L., Arbault, S., Kuhn, A., Sojic, N. ChemElectroChem **3**, 404–409 (2016)
99. Sentic, M., Arbault, S., Goudeau, B., Manojlovic, D., Kuhn, A., Bouffier, L., Sojic, N.: Chem. Commun. **50**, 10202 (2014)
100. Guo, Z., Hao, T., Wang, S., Gan, N., Li, X., Wei, D.: Electrochem. Commun. **14**, 13 (2012)
101. Zhang, M., Dai, W., Yan, M., Ge, S., Yu, J., Song, X., Xu, W.: Analyst **137**, 2112 (2012)
102. Zhang, M., Ge, S., Li, W., Yan, M., Song, X., Yu, J., Xu, W., Huang, J.: Analyst **137**, 680 (2012)
103. Guo, Z., Hao, T., Duan, J., Wang, S., Wei, D.: Talanta **89**, 27 (2012)
104. Liao, N., Zhuo, Y., Chai, Y., Xiang, Y., Cao, Y., Yuan, R., Han, J.: Chem. Commun. **48**, 7610 (2012)
105. Klymenko, O.V., Svir, I., Amatore, C.: ChemPhysChem **14**, 2237 (2013)
106. Deiss, F., LaFratta, C.N., Symer, M., Blicharz, T.M., Sojic, N., Walt, D.R.: J. Am. Chem. Soc. **131**, 6088 (2009)
107. Miao, W., Bard, A.: J. Anal. Chem. **76**, 7109 (2004)
108. Miao, W., Bard, A.: J. Anal. Chem. **76**, 5379 (2004)
109. Habtamu, H.B., Sentic, M., Silvestrini, M., De Leo, L., Not, T., Arbault, S., Manojlovic, D., Sojic, N., Ugo, P.: Anal. Chem. **87**, 12080 (2015)
110. Shen, W., Tian, D., Cui, H., Yang, D., Bian, Z.: Biosens. Bioelectron. **27**, 18 (2011)
111. Sloan, J.H., Siegel, R.W., Ivanova-Cox, Y.T., Watson, D.E., Deeg, M.A., Konrad, R.J.: Clin. Biochem. **45**, 1640 (2012)
112. Wang, G., Jin, F., Dai, N., Zhong, Z., Qing, Y., Li, M., Yuan, R., Wang, D.: Anal. Biochem. **422**, 7 (2012)

113. Yao, X., Yan, P., Tang, Q., Deng, A., Li, J.: Anal. Chim. Acta **798**, 82 (2013)
114. Bertoncello, P.: Front. Biosci.-Landmark **16**, 1084 (2011)
115. Deng, S., Ju, H.: Analyst **138**, 43 (2013)
116. Lei, J., Ju, H.: Trac-Trend Anal. Chem. **30**, 1351 (2011)
117. Lisdat, F., Schaefer, D., Kapp, A.: Anal. Bioanal. Chem. **405**, 3739 (2013)
118. Zhou, H., Gan, N., Li, T., Cao, Y., Zeng, S., Zheng, L., Guo, Z.: Anal. Chim. Acta **746**, 107 (2012)
119. Lin, D., Wu, J., Yan, F., Deng, S., Ju, H.: Anal. Chem. **83**, 5214 (2011)
120. Peng, S., Zhang, X.: Microchim. Acta **178**, 323 (2012)
121. Tian, C.-Y., Zhao, W.-W., Wang, J., Xu, J.-J., Chen, H.-Y.: Analyst **137**, 3070 (2012)
122. Han, E., Ding, L., Lian, H., Ju, H.: Chem. Commun. **46**, 5446 (2010)
123. Li, J., Guo, S., Wang, E.: Rsc Adv. **2**, 3579 (2012)
124. Chai, Y., Tian, D., Wang, W., Cui, H.: Chem. Commun. **46**, 7560 (2010)
125. Tian, D., Zhang, H., Chai, Y., Cui, H.: Chem. Commun. **47**, 4959 (2011)
126. Zhang, Y., Ge, S., Wang, S., Yan, M., Yu, J., Song, X., Liu, W.: Analyst **137**, 2176 (2012)
127. Chikkaveeraiah, B.V., Bhirde, A.A., Morgan, N.Y., Eden, H.S., Chen, X.: ACS Nano **6**, 6546 (2012)
128. Xu, Y., Liu, J., Gao, C., Wang, E.: Electrochem. Commun. **48**, 151 (2014)
129. Wang, T., Zhang, S., Mao, C., Song, J., Niu, H., Jin, B., Tian, Y.: Biosens. Bioelectron. **31**, 369 (2012)
130. Konry, T., Bouhifd, M., Cosnier, S., Whelan, M., Valsesia, A., Rossi, F., Marks, R.S.: Biosens. Bioelectron. **22**, 2230 (2007)
131. Le Goff, A., Holzinger, M., Cosnier, S.: Electrochim. Acta **56**, 3633 (2011)
132. Zamolo, V.A., Valenti, G., Venturelli, E., Chaloin, O., Marcaccio, M., Boscolo, S., Castagnola, V., Sosa, S., Berti, F., Fontanive, G., Poli, M., Tubaro, A., Bianco, A., Paolucci, F., Prato, M.: ACS Nano **6**, 7989 (2012)
133. Dennany, L., Forster, R.J., White, B., Smyth, M., Rusling, J.F.: J. Am. Chem. Soc. **126**, 8835 (2004)
134. Hvastkovs, E.G., So, M., Krishnan, S., Bajrami, B., Tarun, M., Jansson, I., Schenkman, J.B., Rusling, J.F.: Anal. Chem. **2007**, 79 (1897)
135. Liu, Z., Zhou, C., Zheng, B., Qian, L., Mo, Y., Luo, F., Shi, Y., Choi, M.M.F., Xiao, D.: Analyst **136**, 4545 (2011)
136. Sardesai, N.P., Barron, J.C., Rusling, J.F.: Anal. Chem. **83**, 6698 (2011)
137. Li, L., Chen, Y., Lu, Q., Ji, J., Shen, Y., Xu, M., Fei, R., Yang, G., Zhang, K., Zhang, J.-R., Zhu, J.-J.: Sci. Rep. **3** (2013)
138. Li, W., Li, L., Li, M., Yu, J., Ge, S., Yan, M., Song, X.: Chem. Commun. **49**, 9540 (2013)
139. Li, Z., Wang, Y., Kong, W., Li, C., Wang, Z., Fu, Z.: Biosens. Bioelectron. **39**, 311 (2013)
140. Burton, P.R., Clayton, D.G., Cardon, L.R., Craddock, N., Deloukas, P., Duncanson, A., Kwiatkowski, D.P., McCarthy, M.I., Ouwehand, W.H., Samani, N.J., Todd, J.A., Donnelly, P., Barrett, J.C., Davison, D., Easton, D., Evans, D., Leung, H.-T., Marchini, J.L., Morris, A.P., Spencer, C.C.A., Tobin, M.D., Attwood, A.P., Boorman, J.P., Cant, B., Everson, U., Hussey, J.M., Jolley, J.D., Knight, A.S., Koch, K., Meech, E., Nutland, S., Prowse, C.V., Stevens, H.E., Taylor, N.C., Walters, G.R., Walker, N.M., Watkins, N.A., Winzer, T., Jones, R.W., McArdle, W.L., Ring, S.M., Strachan, D.P.; Pembrey, M., Breen, G., St. Clair, D., Caesar, S., Gordon-Smith, K., Jones, L., Fraser, C., Green, E.K., Grozeva, D., Hamshere, M.L., Holmans, P.A., Jones, I.R., Kirov, G., Moskvina, V., Nikolov, I., O'Donovan, M.C., Owen, M.J., Collier, D.A., Elkin, A., Farmer, A., Williamson, R., McGuffin, P., Young, A.H., Ferrier, I.N., Ball, S.G., Balmforth, A.J., Barrett, J.H., Bishop, D.T., Iles, M.M., Maqbool, A., Yudasheve, N., Hall, A.S., Braund, P.S.; Dixon, R.J., Mangino, M., Stevens, S., Thompson, J.R., Bredin, F., Tremelling, M., Parkes, M., Drummond, H., Lees, C.W., Nimmo, E.R., Satsangi, J., Fisher, S.A., Forbes, A., Lewis, C.M., Onnie, C.M., Prescott, N.J., Sanderson, J., Mathew, C.G., Barbour, J., Mohiuddin, M.K., Todhunter, C.E., Mansfield, J.C., Ahmad, T., Cummings, F.R., Jewell, D.P.: Nature **447**, 661 (2007)

141. McCarthy, J.J., Hilfiker, R.: Nat. Biotechnol. **18**, 505 (2000)
142. Sun, B., Qi, H., Ma, F., Gao, Q., Zhang, C., Miao, W.: Anal. Chem. **82**, 5046 (2010)
143. Wang, S., Milam, J., Ohlin, A.C., Rambaran, V.H., Clark, E., Ward, W., Seymour, L., Casey, W.H., Holder, A.A., Miao, W.: Anal. Chem. **81**, 4068 (2009)
144. Ding, C., Zhang, W., Wang, W., Chen, Y., Li, X.: Trac-Trend Anal. Chem. **65**, 137 (2015)
145. Jiang, J., Chai, Y., Cui, H.: Rsc Adv. **1**, 247 (2011)
146. Jiang, D., Liu, F., Liu, C., Liu, L., Li, Y., Pu, X.: Anal. Meth. **6**, 1558 (2014)
147. Chen, Y., Xu, J., Su, J., Xiang, Y., Yuan, R., Chai, Y.: Anal. Chem. **84**, 7750 (2012)
148. Liu, T., Chen, X., Hong, C.-Y., Xu, X.-P., Yang, H.-H.: Microchim. Acta **181**, 731 (2014)
149. Wang, J., Zhao, W.-W., Zhou, H., Xu, J.-J., Chen, H.-Y.: Biosens. Bioelectron. **41**, 615 (2013)
150. Wei, W., Zhou, J., Li, H., Yin, L., Pu, Y., Liu, S.: Analyst **138**, 3253 (2013)
151. Zhou, H., Liu, J., Xu, J.-J., Chen, H.-Y.: Chem. Commun. **47**, 8358 (2011)
152. Zhou, H., Liu, J., Xu, J.-J., Chen, H.-Y.: Anal. Chem. **83**, 8320 (2011)
153. Dennany, L., Forster, R.J., Rusling, J.F.: J. Am. Chem. Soc. **125**, 5213 (2003)
154. Lee, J.H., Yigit, M.V., Mazumdar, D., Lu, Y.: Adv. Drug Deliv. Rev. **62**, 592 (2010)
155. Zhou, W., Huang, P.-J.J., Ding, J., Liu, J.: Analyst **139**, 2627 (2014)
156. Liu, Z., Zhang, W., Hu, L., Li, H., Zhu, S., Xu, G.: Chem. Eur. J. **16**, 13356 (2010)
157. Hu, L., Bian, Z., Li, H., Han, S., Yuan, Y., Gao, L., Xu, G.: Anal. Chem. **81**, 9807 (2009)
158. Chen, Y., Jiang, B., Xiang, Y., Chai, Y., Yuan, R.: Chem. Commun. **47**, 7758 (2011)
159. Chen, L., Cai, Q., Luo, F., Chen, X., Zhu, X., Qiu, B., Lin, Z., Chen, G.: Chem. Commun. **46**, 7751 (2010)
160. Dang, J., Guo, Z., Zheng, X.: Anal. Chem. **86**, 8943 (2014)
161. Yuan, T., Liu, Z., Hu, L., Zhang, L., Xu, G.: Chem. Commun. **47**, 11951 (2011)
162. Shi, H.-W., Wu, M.-S., Du, Y., Xu, J.-J., Chen, H.-Y.: Biosens. Bioelectron. **55**, 459 (2014)
163. Tian, C.-Y., Xu, J.-J., Chen, H.-Y.: Chem. Commun. **48**, 8234 (2012)
164. Hu, L., Xu, G.: Chem. Soc. Rev. **39**, 3275 (2010)
165. Wilson, R., Kremeskötter, J., Schiffrin, D.J., Wilkinson, J.S.: Biosens. Bioelectron. **11**, 805 (1996)
166. de Poulpiquet, A., Diez-Buitrago, B., Milutinovic, M., Sentic, M., Arbault, S., Bouffier, L., Kuhn, A., Sojic, N.: (2016, submitted)
167. Marquette, C.A., Blum, L.J.: Anal. Chim. Acta **1** (1999)
168. Marquette, C.A., Degiuli, A., Blum, L.J.: Biosens. Bioelectron. **19**, 433 (2003)
169. Leca, B., Blum, L.J.: Analyst **125**, 789 (2000)
170. Wang, X.F., Zhou, Y., Xu, J.J., Chen, H.Y.: Adv. Funct. Mater. **19**, 1444 (2009)
171. Dai, H., Wu, X., Xu, H., Wei, M., Wang, Y., Chen, G.: Electrochem. Comm. **11**, 1599 (2009)
172. Liu, X., Ju, H.: Anal. Chem. **80**, 5377 (2008)
173. Jameison, F., Sanchez, R.I., Dong, L., Leland, J.K., Yost, D., Martin, M.T.: Anal. Chem. **68**, 1298 (1996)
174. Loget, G., Kuhn, A.: Nat. Commun. **2**, 535 (2011)
175. Roche, J., Carrara, S., Lannelongue, J., Loget, G., Bouffier, L., Kuhn, A., Sanchez, J., Fischer, P.: Sci. Rep. **4**, 6705 (2014)
176. Delaney, J.L., Hogan, C.F., Tian, J., Shen, W.: Anal. Chem. **83**, 1300 (2011)
177. Doeven, E.H., Barbante, G.J., Kerr, E., Hogan, C.F., Endler, J.A., Francis, P.S.: Anal. Chem. **86**, 2727 (2014)
178. Swanick, K.N., Ladouceur, S., Zysman-Colman, E., Ding, Z.: Angew. Chem. Int. Ed. **51**, 11079 (2012)
179. Doeven, E.H., Barbante, G.J., Hogan, C.F., Francis, P.S.: Chempluschem **80**, 456 (2015)
180. Valenti, G., Rampazzo, E., Bonacchi, S., Khajvand, T., Juris, R., Montalti, M., Marcaccio, M., Paolucci, F., Prodi, L.: Chem. Commun. **48**, 4187 (2012)

181. Zanarini, S., Felici, M., Valenti, G., Marcaccio, M., Prodi, L., Bonacchi, S., Contreras-Carballada, P., Williams, R.M., Feiters, M.C., Nolte, R.J.M., De Cola, L., Paolucci, F.: Chem. Eur. J. **17**, 4640 (2011)
182. Zanarini, S., Rampazzo, E., Ciana, L.D., Marcaccio, M., Marzocchi, E., Montalti, M., Paolucci, F., Prodi, L.: J. Am. Chem. Soc. **131**, 2260 (2009)
183. Zanarini, S., Rampazzo, E., Bonacchi, S., Juris, R., Marcaccio, M., Montalti, M., Paolucci, F., Prodi, L.: J. Am. Chem. Soc. **131**, 14208 (2009)